

# Prague Medical REPORT

(Sborník lékařský)

Multidisciplinary Biomedical Journal  
of the First Faculty of Medicine,  
Charles University

Vol. 123 (2022) No. 1

## Primary Scientific Studies

Effect of Inferior Alveolar Nerve Transection on the Inorganic Component of Molars of Rat Mandible / *Němec I., Smrčka V., Mihaljevič M., Hill M., Pokorný J., Páral V., Pračková I.* page 5

Endoscopic Resection of Upper Gastrointestinal Subepithelial Tumours: Our Clinical Experience and Results / *Zeki Buldanlı M., Yener O.* page 20

## Case Reports

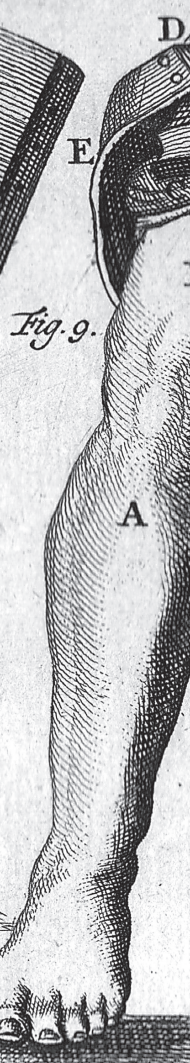
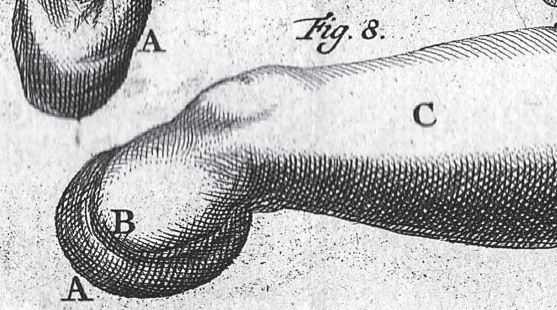
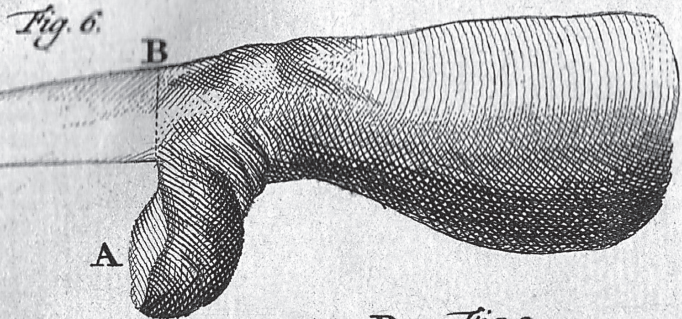
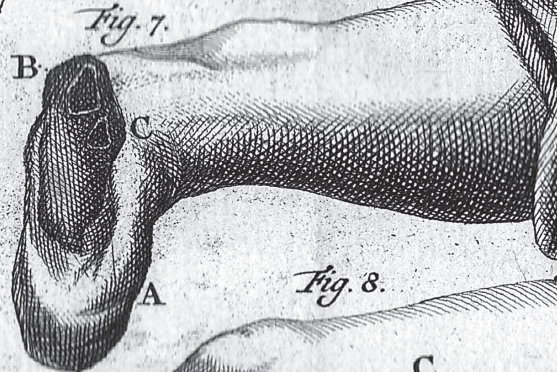
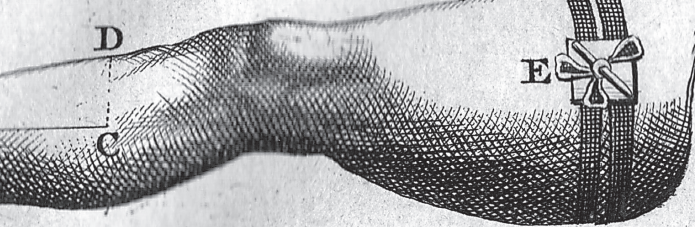
POEMS Syndrome Diagnosis in a Patient with Mixed Polyneuropathy: Case Report / *Ocampo-Navia M. I., Negret Noreña M. A., Chaparro Santos L. R., Morera Afanador J. R., Quintero Farías R. A., Bustos Sánchez J. L.* page 27

Effective Treatment of a Melanoma Patient with Hemophagocytic Lymphohistiocytosis after Nivolumab and Ipilimumab Combined Immunotherapy / *Pacholczak-Madej R., Grela-Wojewoda A., Lompart J., Żuchowska-Vogelgesang B., Ziobro M.* page 35

Pneumomediastinum: A Rare Complication of Endobronchial Ultrasound Guided Fine Needle Aspiration / *Saha B. K.* page 43

Parvovirus B19 Intrauterine Infection and Eventration of the Diaphragm / *Mitsiakos G., Gavras C., Katsaras G. N., Chatziioannidis I., Mouravas V., Mitsiakou C., Lampropoulos V., Nikolaidis N.* page 48

**Instructions to Authors** page 56



**Prague Medical Report (Prague Med Rep) is indexed and abstracted by Index-medicus, MEDLINE, PubMed, EuroPub, CNKI, DOAJ, EBSCO, and Scopus.**

**Abstracts and full-texts of published papers can be retrieved from the World Wide Web (<https://pmr.lf1.cuni.cz>).**

# Effect of Inferior Alveolar Nerve Transection on the Inorganic Component of Molars of Rat Mandible

**Ivo Němec<sup>1</sup>, Václav Smrčka<sup>2</sup>, Martin Mihaljevič<sup>3</sup>, Martin Hill<sup>4</sup>,  
Jaroslav Pokorný<sup>5</sup>, Václav Páral<sup>6</sup>, Ivana Pračková<sup>6,7</sup>**

<sup>1</sup>Department of Otorhinolaryngology and Maxillofacial Surgery, Third Faculty of Medicine, Charles University and Military University Hospital Prague, Prague, Czech Republic;

<sup>2</sup>Institute for History of Medicine and Foreign Languages, First Faculty of Medicine, Charles University, Prague, Czech Republic; Department of Plastic Surgery, First Faculty of Medicine, Charles University and Na Bulovce Hospital, Prague, Czech Republic;

<sup>3</sup>Institute of Geochemistry, Mineralogy and Mineral Resources, Faculty of Science, Charles University, Prague, Czech Republic;

<sup>4</sup>Institute of Endocrinology, Prague, Czech Republic;

<sup>5</sup>Institute of Physiology, First Faculty of Medicine, Charles University, Prague, Czech Republic;

<sup>6</sup>Department of Anatomy, Histology and Embryology, Faculty of Veterinary Medicine, University of Veterinary and Pharmaceutical Sciences Brno, Brno, Czech Republic;

<sup>7</sup>Department of Anatomy, Faculty of Medicine, Masaryk University, Brno, Czech Republic

Received March 9, 2021; Accepted January 31, 2022.

**Key words:** Inferior alveolar nerve – Molars of mandible – Rats – Elements – Nerve transection

*Part of the equipment used for the study was purchased from the Operational Programme Prague – Competitiveness (Project CZ.2.16/3.1.00/21516). Supported with grant Progres Q35/LF1.*

**Mailing Address:** Ivo Němec, MD., Department of Otorhinolaryngology and Maxillofacial Surgery, Third Faculty of Medicine, Charles University and Military University Hospital Prague, U Vojenské nemocnice 1200, 169 02 Prague 6, Czech Republic; e-mail: Ivo.Nemec@uvm.cz

**Abstract:** The objective of the study was to determine the effects of inferior alveolar nerve transection on inorganic components in mandibular molars of the rat. We used 26 male laboratory rats of the Wistar strain for the study, age 7–9 weeks. The rats were divided in three groups. The control group (intact) included 6 rats. The surgery was performed under general anesthesia. The experimental group included (group with the nerve transected on the left) included 12 rats. The sham group (group with the nerve prepared without transection) included 8 rats. The animals were sacrificed after 4 weeks. Molars from the left and right sides of the mandible were extracted. Element content levels were determined using inductively coupled plasma mass spectrometry. The following elements were determined in all samples: magnesium (Mg), sodium (Na), potassium (K), calcium (Ca), zinc (Zn), and strontium (Sr). The nerve transection caused: a reduction of the contents of Ca and Sr in the mandibular molars; an increase in the contents of Mg and Zn; a difference arrangement of both sides for Na. The surgery approach itself caused a decrease in the contents of Na and K in the experimental and sham groups; the difference in K in M3 between the left and right sides disappeared due to the surgery. Our results have confirmed the hypothesis of inferior alveolar nerve transection having an effect on inorganic components in mandibular molars in the rat.

## Introduction

The pulp is innervated by sensory nerve fibers, forming the subodontoblastic plexus and continuing into the odontoblast layer and dentinal tubules (Berkovitz, 2016) as free nerve endings (Fristad, 1997). The nerve supply of the dentin-pulp complex is mainly made up of A fibers (both delta and beta) and C fibers. They are classified according to their diameter and their conduction velocity. The A fibers are mainly stimulated by an application of cold, producing sharp pain, whereas stimulation of the C fibers produces a dull aching pain. Because of their location and arrangement, the C fibers are responsible for referred pain (Abd-Elmeguid and Yu, 2009). Furthermore, the pulp is innervated by vasoconstrictor sympathetic nerve fibres (Berkovitz, 2016).

Nerve endings contained in the pulp release various neuropeptides with an impact on the homeostasis (Fristad, 1997; Byers et al., 2003; Berkovitz, 2016). As reported by Jacobsen and Heyeraas (1996), neuropeptides such as CGRP (calcitonin gene-related peptide) and substance P are involved in dentin production. The authors have published information on the effects of capsaicin and of a transection of the inferior alveolar nerve (IAN) on first molar dentin production in the rat. As follows from the study, capsaicin reduced CGRP- and substance P-immunoreactive fibrils in the pulp. A transection of the IAN resulted in an almost complete loss of immunoreactive fibrils in the pulp. Dentin production was reduced in both groups compared to the control (Jacobsen and Heyeraas, 1996).

IAN injury can occur in the fracture of the mandible (Singh et al., 2016), in various surgical procedures in the mandible or in the course of endodontic treatment

(Baxmann, 2006; Ozkan et al., 2008). IAN lesion can be caused by a pathological process (Ozkan et al., 2008). This nerve damage may be either temporary or permanent (Bhat and Cariappa, 2012).

The teeth (enamel, dentin and cementum) contain organic and inorganic components (Abou Neel et al., 2016). Calcium is one of essential elements in the teeth. Calcium is found there in the form of hydroxyapatite, which also includes phosphorus (Dermience et al., 2015). Calcium metabolism disorders are reflected in changes of tooth structure and properties (Wilhelm, 2007). Various studies have focused on analyzing chemical elements present in the teeth (Curzon and Crocker, 1978; Curzon and Cutress, 1983; Vrbič et al., 1987; Lane and Peach, 1997; Reitznerová et al., 2000; Fischer et al., 2009, 2013; Ghadimi et al., 2013). Curzon and Crocker (1978) studied trace elements with respect to caries; as found by these authors, fluorine, aluminium, iron, selenium and strontium are associated with a low risk of developing caries, while manganese, copper and cadmium are associated with a high risk.

Minimum information on the effects of sensory innervation on inorganic components of tooth structure is found in the literature (Němec et al., 2018a).

In our previous study, we have determined 14 elements in the bone and teeth of the mandible of rat (magnesium, sodium, potassium, calcium, manganese, iron, cobalt, nickel, copper, zinc, rubidium, strontium, molybdenum and barium) (Němec et al., 2018b).

For the purposes of this study, we analysed the following elements: magnesium (Mg), sodium (Na), potassium (K), calcium (Ca), zinc (Zn), and strontium (Sr).

A change of inorganic components of tooth structure due to an innervation disorder can be manifested by altered properties of the given tissue. The objective of the study was to determine the effects of IAN transection on inorganic components in mandibular molars of the rat.

## Material and Methods

### *Experimental animals*

We used 26 male laboratory rats of the Wistar strain, age 7–9 weeks and weight 320–405 g. The animals were obtained from the breeding colony of the Institute of Physiology of the First Faculty of Medicine, Charles University, Prague. The experiment was performed in compliance with applicable guidelines for the use of laboratory animals – EU Council Directive 86/609/EEC. The animals were kept in boxes at 20–23 °C, using the standard 12-hour light/12-hour dark cycle. The animals received a normal diet and had water available *ad libitum*. The rats were divided in three groups. The control group (group-C, intact) included 6 rats; the experimental group (group-E, with the nerve transected on the left) included 12 rats; and the sham group (group-S, with the nerve prepared without transection) included 8 rats.

### *Transection of the inferior alveolar nerve*

The surgery was performed under general anesthesia induced using intraperitoneal administration of thiopental 4 mg/100 g of rat weight. A microsurgical technique was used to approach and excise the nerve (used microscope: Carl Zeiss OPTON S4, Germany). An incision in the left face was used to expose the masseter muscle fascia, which was cut in the direction of muscle fascicles between the facial nerve and the parotid duct. After preparing the muscles, we reached the lateral part of the mandible at the place of its prominence (*tuberculum massetericum*). The bone crest (*crista masseterica*) was identified in the direction from the prominence to the condylar process (*processus condylaris*). Caudally from the prominence, we used a round dental milling cutter sized 1.2 mm (N 500.104.001.001.012 TC, Medin, a.s., Nové Město na Moravě) to remove a part of the bone and expose the neurovascular bundle in the range of 3 mm. The nerve was slightly pulled out from the mandibular canal and excised in the range of 3 mm. The neurovascular bundle was prepared using a microsurgical technique. This procedure enabled us to avoid causing any injury to blood vessels while excising the part of the nerve. The wound was rinsed with 1 ml of saline solution. Edges of the muscle were adapted using one non-absorbable suture. The same non-absorbable material was used to close the skin.

### *Animal killing and extraction of the molars*

Four weeks later, the animals were weighted and killed by overdosing with thiopental using intraperitoneal administration. Individual molars (M1, M2, and M3) were gradually extracted from the mandible (on both sides). The teeth were mechanically cleaned and rinsed in *aqua pro injectione*.

### *Chemical analysis*

The weighted amount of 10–20 mg of the dried samples of individual molars were inserted to 10 ml volumetric flasks; a value of 0.5 ml of concentrated HNO<sub>3</sub> was added; subsequently, the samples were dissolved by careful heating of the glass on the heating plate at approx. 100 °C. After cooling, deionized water was added to the mark of the volumetric flask. Blank samples were prepared for every series of 20 samples. The measurement quality was tested by analyzing the standard reference material (SRM 1400, Bone Ash, National Institute of Standards and Technology, Gaithersburg, MD). Differences between the measured and certified values were lower than the 10% RSD (relative standard deviation). All the acids used in the dissolution procedure were reagent grade (Merck, Darmstadt, Germany). Deionized water from MilliQPlus (Millipore, Billerica, MA) were used to prepare the solutions. The contents of Mg, Na, K, Ca, Zn, and Sr in the solutions were determined using inductively coupled plasma mass spectrometry (ICP MS, X Series II, Fisher Scientific, GmbH, Bremen, Germany) under the following conditions: ICP 1350 W, “peak jump” measurement mode, measurement time 3×50 s, ion optics parameters optimized

with Ge, Rh, and Re 20 µg/l solutions (Astasol, Analytika, Czech Republic), gas flows 13.5 l/min (cooling), 0.7 l/min (auxiliary), 0.65 l/min (nebulizer). Measured isotopes of  $^{72}\text{Ge}$ ,  $^{103}\text{Rh}$ ,  $^{185}\text{Re}$ , were used as internal standards.

#### *Statistical analysis*

- 1) The comparison of mean weight increase of the animals after 4 weeks among the groups was done using the Kruskal-Wallis test.
- 2) Respecting the skewed distribution and non-constant variance in most dependent variables, these were transformed by power transformations to data symmetry and homoscedasticity prior further processing (Meloun et al., 2000). The homogeneity and distribution of the transformed data and residuals was checked by residual analysis as described elsewhere (Meloun et al., 2002, 2004). The model consisted of Subject factor explaining inter-individual variability, between-subject factor Group (control [C], experimental [E], sham [S]), within-subject factors Location (three sites were investigated in animal such as M1, M2, and M3) and factor Side (right [R] vs. left [L]), and all corresponding interaction between the factors except of the subject factor. For instance, significant Group×Location interaction indicates that the Group factor significantly influences the arrangement of differences between location of sampling sites. Statistical software Statgraphics Centurion, version 18 from Statgraphics Technologies, Inc. (The Plains, Virginia, USA) was used for the statistical analysis.

The null hypotheses in all factors and all possible between-factor interactions were tested. However, the primary questions were associated with null hypotheses for the interactions as follows: factor difference between groups, Group×Location, Side×Group, Side×Location, and Side×Group×Location.

## **Results**

#### *Change in animal weight*

No statistically significant differences in weight gain of the animals were shown between individual groups during the observation period (4 weeks).

#### *Analyzed elements*

Six elements were analyzed in all groups: Mg, Na, K, Ca, Zn, and Sr.

#### *Change in element contents in mandibular molars (M1–3)*

The content of **Mg** in group-C is lower compared to group-E and group-S. At the same time, there is a difference between group-E and group-S. A difference between the left and right sides was observed only in group-S (Figure 1).

For **Na**, the content is lower in group-E and group-S compared to group-C. In group-E, the arrangement of the left and right sides differed from group-C and group-S (Figure 2).

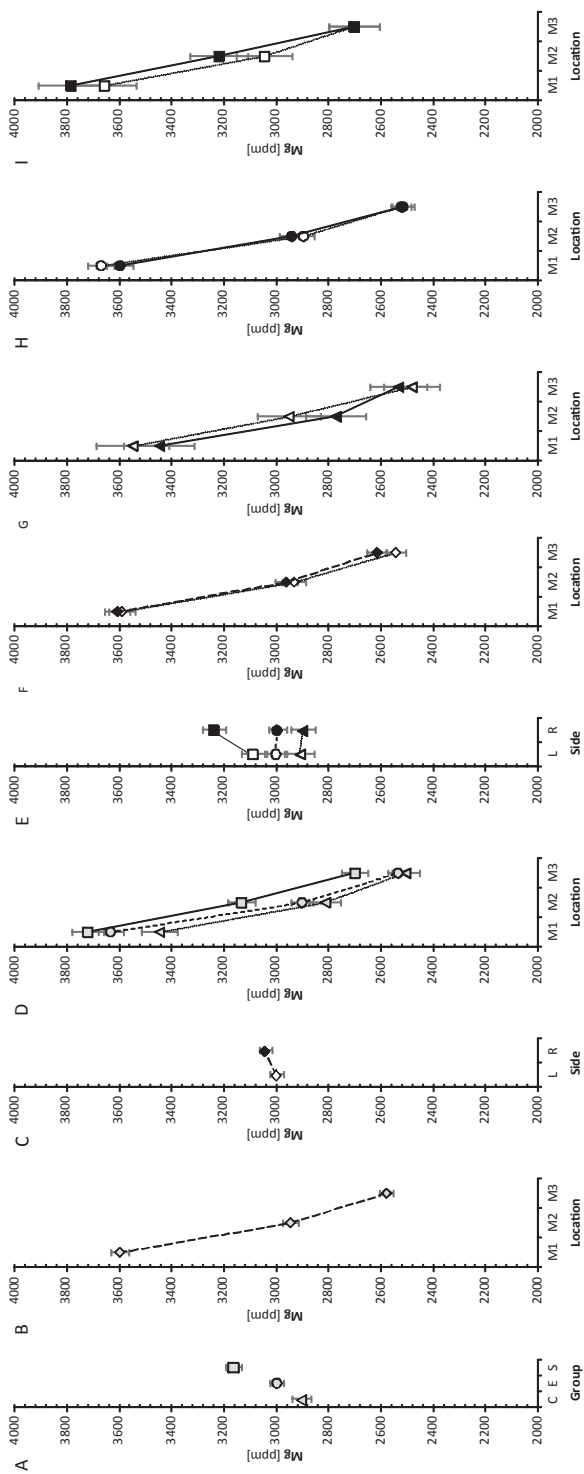


Figure 1 – The relationships between concentrations of Mg (ppm) in groups, location of sampling sites, and side of sampling were evaluated using ANOVA model. The model consisted of Subject factor explaining inter-individual variability, between-subject factor Group (control [C], experimental [E], sham group [S]), within-subject factors Location (three sites were investigated in animal such as M1, M2, and M3) and factor Side (right [R] vs. left [L]), and all corresponding interaction between the factors except of the subject factor. F represents the Fisher's statistic and p designates statistical significance for the factors and interaction. The symbols with error bars represent re-transformed means with their 95% confidence intervals (triangles, circles, and squares symbolize C, E, and S group, respectively, while the diamonds the summary for all groups). The full and empty symbols represent right and left side of sampling, respectively, while the grey ones the summary for both sides. The 95% confidence intervals are computed using the least significant difference multiple comparisons ( $p < 0.05$ ). The confidence intervals, which do not overlap each other, denote significant difference between the respective subgroup means. Statistical software Statgraphics Centurion, version 18 from Statgraphics Technologies, Inc. (The Plains, Virginia, USA) was used for the statistical analysis.

All – Group:  $F = 32.1, p < 0.001$  (Panel A); Location:  $F = 534.7, p < 0.001$  (Panel B); Side:  $F = 2.7, p = 0.101$  (Panel C); Group  $\times$  Location:  $F = 1.9, p = 0.119$  (Panel D); Group  $\times$  Side:  $F = 4.1, p = 0.019$  (Panel E); Location  $\times$  Side:  $F = 0.6, p = 0.554$  (Panel F); Group  $\times$  Location  $\times$  Side:  $F = 0.4, p = 0.81$ ; Subj(Group):  $F = 31.8, p < 0.001$ .

Group C – Location:  $F = 72, p < 0.001$ ; Side:  $F = 1.1, p = 0.296$ ; Location  $\times$  Side:  $F = 1.1, p = 0.353$  (Panel G); Subj:  $F = 14.7, p < 0.001$ .

Group E – Location:  $F = 626.2, p < 0.001$ ; Side:  $F = 0.1, p = 0.781$ ; Location  $\times$  Side:  $F = 1.5, p = 0.23$  (Panel H); Subj:  $F = 59.2, p < 0.001$ .

Group S – Location:  $F = 89.4, p < 0.001$ ; Side:  $F = 2.4, p = 0.133$ ; Location  $\times$  Side:  $F = 0.7, p = 0.507$  (Panel I); Subj:  $F = 15.1, p < 0.001$ .

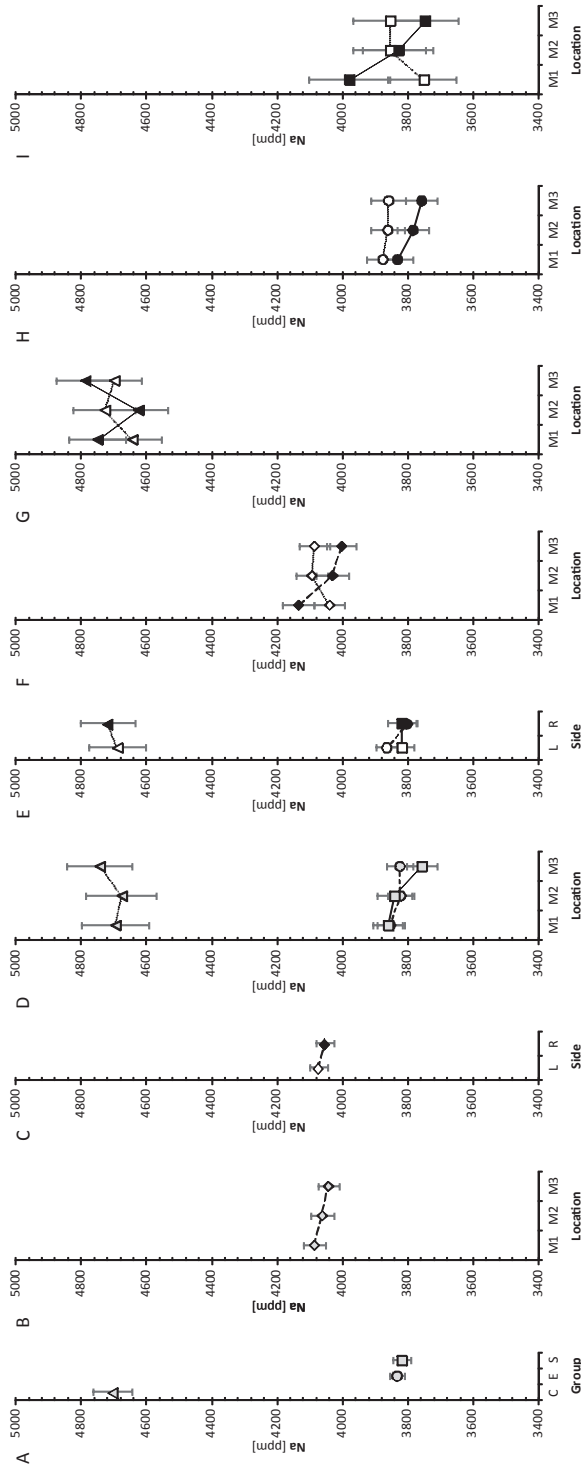


Figure 2 – The relationships between concentrations of Na (ppm) in groups, location of sampling sites, and side of sampling were evaluated using ANOVA model. The drawings and symbols are the same as for Figure 1.

All – Group:  $F=297.1$ ,  $p<0.001$  (Panel A); Location:  $F=0.8$ ,  $p=0.441$  (Panel B); Side:  $F=0.4$ ,  $p=0.513$  (Panel C); Group×Location:  $F=1.1$ ,  $p=0.382$  (Panel D); Group×Side:  $F=1.2$ ,  $p=0.295$  (Panel E); Location×Side:  $F=4.3$ ,  $p=0.017$  (Panel F); Group×Location×Side:  $F=3.1$ ,  $p=0.019$ ; Subj(Group):  $F=28.3$ ,  $p<0.001$ .  
 Group C – Location:  $F=0.7$ ,  $p=0.531$ ; Side:  $F=0.3$ ,  $p=0.57$ ; Location×Side:  $F=1.8$ ,  $p=0.197$  (Panel G); Subj:  $F=89.5$ ,  $p<0.001$ .  
 Group E – Location:  $F=0.9$ ,  $p=0.406$ ; Side:  $F=6.7$ ,  $p=0.013$ ; Location×Side:  $F=0.4$ ,  $p=0.706$  (Panel H); Subj:  $F=28.8$ ,  $p<0.001$ .  
 Group S – Location:  $F=0.3$ ,  $p=0.714$ ; Side:  $F=0.2$ ,  $p=0.638$ ; Location×Side:  $F=2.6$ ,  $p=0.086$  (Panel I); Subj:  $F=13.9$ ,  $p<0.001$ .

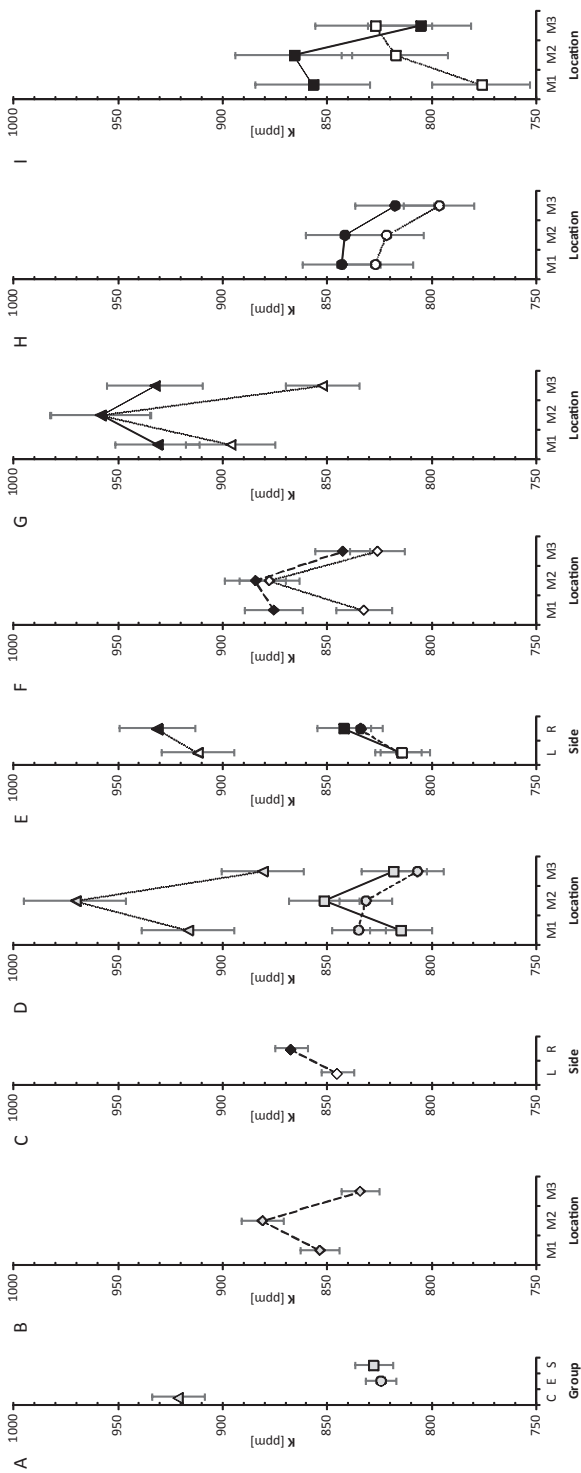


Figure 3 – The relationships between concentrations of K (ppm) in groups, location of sampling sites, and side of sampling were evaluated using ANOVA model. The drawings and symbols are the same as for Figure 1.

All – Group:  $F=52.4, p<0.001$  (Panel A); Location:  $F=11.6, p<0.001$  (Panel B); Side:  $F=7.8, p=0.006$  (Panel C); Group  $\times$  Location:  $F=2.4, p=0.058$  (Panel D); Group  $\times$  Side:  $F=0.2, p=0.822$  (Panel E); Location  $\times$  Side:  $F=1.9, p=0.154$  (Panel F); Group  $\times$  Location  $\times$  Side:  $F=3.5, p=0.01$ ; Subj(Group):  $F=33.8, p<0.001$ .  
 Group C – Location:  $F=10.8, p<0.001$ ; Side:  $F=10.6, p=0.004$ ; Location  $\times$  Side:  $F=4.3, p=0.028$  (Panel G); Subj:  $F=105.3, p<0.001$ .  
 Group E – Location:  $F=2.9, p=0.065$ ; Side:  $F=3.4, p=0.072$ ; Location  $\times$  Side:  $F=0, p=0.973$  (Panel H); Subj:  $F=44, p<0.001$ .  
 Group S – Location:  $F=1.3, p=0.281$ ; Side:  $F=5.8, p=0.022$ ; Location  $\times$  Side:  $F=4.2, p=0.024$  (Panel I); Subj:  $F=4.3, p=0.002$ .

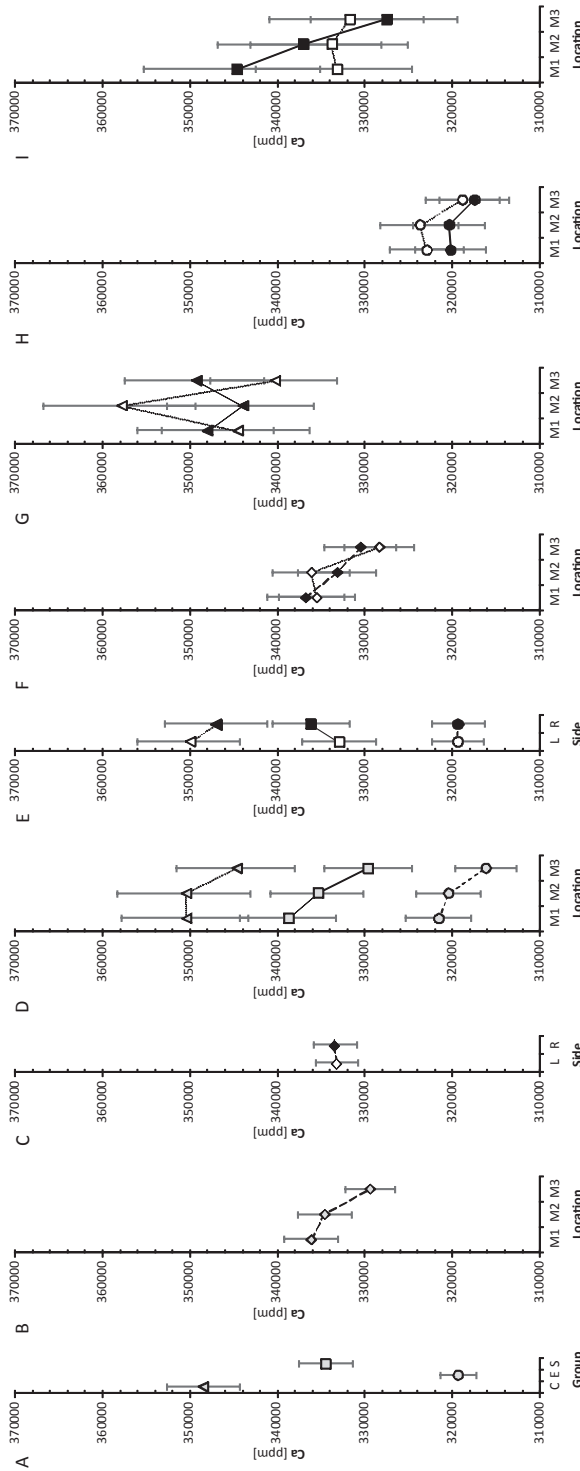


Figure 4 – The relationships between concentrations of Ca (ppm) in groups, location of sampling sites, and side of sampling were evaluated using ANOVA model.

The drawings and symbols are the same as for Figure 1.

All – Group:  $F=48.3, p<0.001$  (Panel A); Location:  $F=2.7, p=0.069$  (Panel B); Side:  $F=0, p=0.942$  (Panel C); Group×Location:  $F=0.1, p=0.988$  (Panel D); Group×Side:  $F=0.4, p=0.669$  (Panel E); Location×Side:  $F=0.4, p=0.678$  (Panel F); Group×Location × Side:  $F=1.2, p=0.315$ ; Subj(Group):  $F=9.3, p<0.001$ .  
 Group C – Location:  $F=0.6, p=0.545$ ; Side:  $F=0, p=0.967$ ; Location×Side:  $F=2.3, p=0.126$  (Panel G); Subj:  $F=11.3, p<0.001$ .  
 Group E – Location:  $F=1, p=0.36$ ; Side:  $F=1.1, p=0.311$ ; Location×Side:  $F=0.1, p=0.949$  (Panel H); Subj:  $F=7.9, p<0.001$ .  
 Group S – Location:  $F=1.1, p=0.35$ ; Side:  $F=0.4, p=0.532$ ; Location×Side:  $F=0.8, p=0.481$  (Panel I); Subj:  $F=14.3, p<0.001$ .

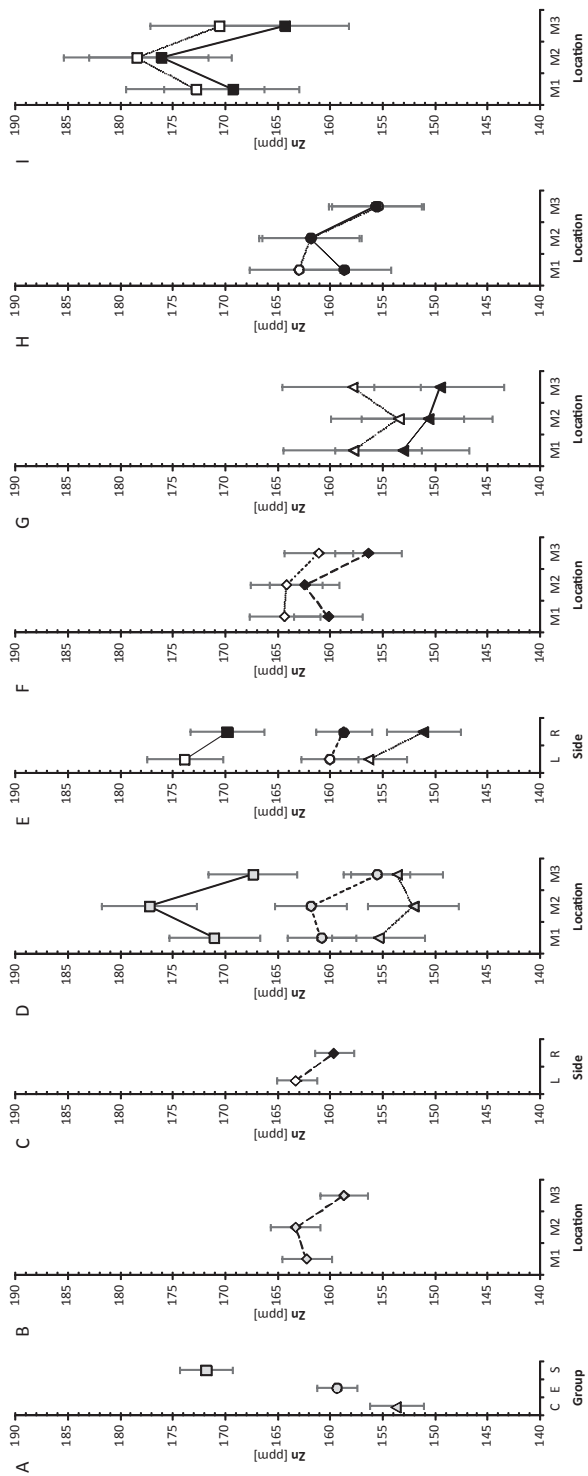


Figure 5 – The relationships between concentrations of Zn (ppm) in groups, location of sampling sites, and side of sampling were evaluated using ANOVA model. The drawings and symbols are the same as for Figure 1.

All – Group:  $F=27.8, p<0.001$  (Panel A); Location:  $F=2.1, p=0.126$  (Panel B); Side:  $F=3.5, p=0.065$  (Panel C); Group×Location:  $F=1, p=0.431$  (Panel D); Group×Side:  $F=0.4, p=0.651$  (Panel E); Location×Side:  $F=0.2, p=0.785$  (Panel F); Group×Location×Side:  $F=0.2, p=0.941$ ; Subj(Group):  $F=16.1, p<0.001$ .

Group C – Location:  $F=0.3, p=0.751$ ; Side:  $F=2.2, p=0.153$ ; Location×Side:  $F=0.2, p=0.821$  (Panel G); Subj:  $F=9.1, p<0.001$ .

Group E – Location:  $F=2.2, p=0.119$ ; Side:  $F=0.3, p=0.61$ ; Location×Side:  $F=0.3, p=0.738$  (Panel H); Subj:  $F=19.8, p<0.001$ .

Group S – Location:  $F=2.4, p=0.109$ ; Side:  $F=1.2, p=0.282$ ; Location×Side:  $F=0.1, p=0.895$  (Panel I); Subj:  $F=15.5, p<0.001$ .

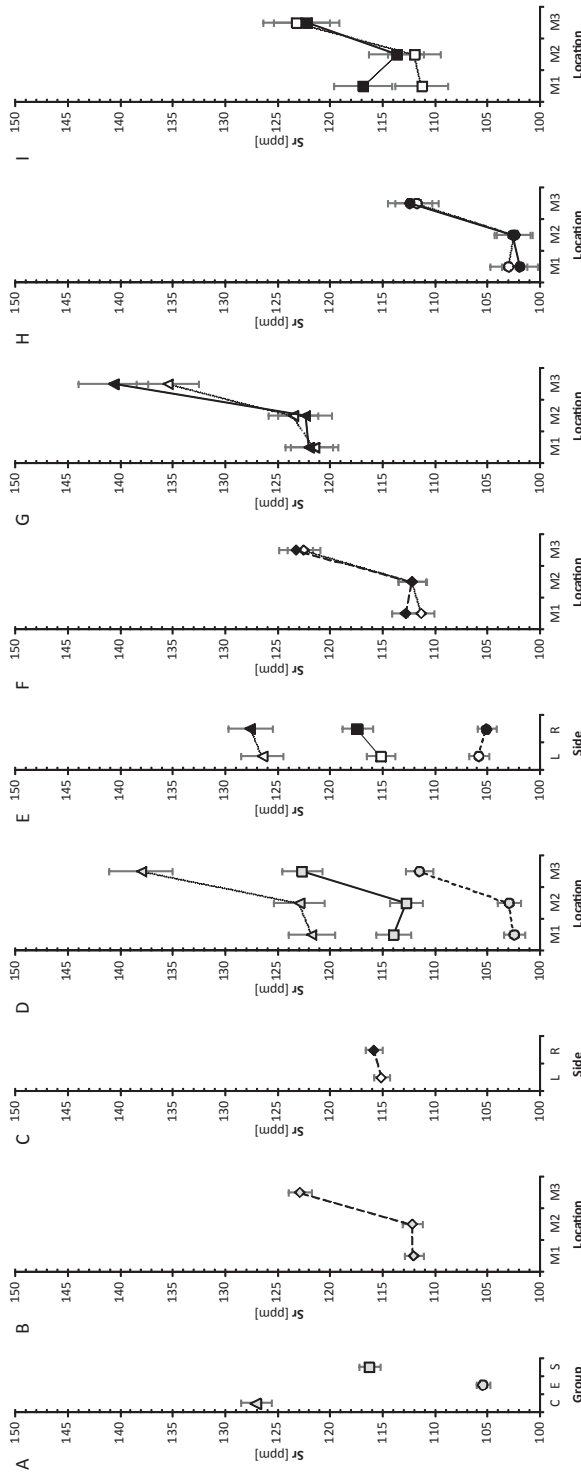


Figure 6 – The relationships between concentrations of Sr (ppm) in groups, location of sampling sites, and side of sampling were evaluated using ANOVA model. The drawings and symbols are the same as for Figure 1.

All – Group:  $F=246.7, p<0.001$  (Panel A); Location:  $F=73.3, p<0.001$  (Panel B); Side:  $F=0.8, p=0.369$  (Panel C); Group×Location:  $F=0.7, p=0.614$  (Panel D); Group×Side:  $F=1.6, p=0.208$  (Panel E); Location×Side:  $F=0.4, p=0.704$  (Panel F); Group×Location×Side:  $F=1.2, p=0.336$ ; Subj(Group):  $F=36.1, p<0.001$ .  
 Group C – Location:  $F=47.4, p<0.001$ ; Side:  $F=0.6, p=0.434$ ; Location×Side:  $F=1.2, p=0.32$  (Panel G); Subj:  $F=3.4, p=0.018$ .  
 Group E – Location:  $F=34.2, p<0.001$ ; Side:  $F=0, p=0.917$ ; Location×Side:  $F=0.2, p=0.791$  (Panel H); Subj:  $F=24, p<0.001$ .  
 Group S – Location:  $F=14.7, p<0.001$ ; Side:  $F=2.1, p=0.161$ ; Location×Side:  $F=1.5, p=0.228$  (Panel I); Subj:  $F=54.3, p<0.001$ .

For **K**, the content is lower in group-E and group-S compared to group-C. In group-C, a difference was observed between the left and right sides in M3; in group-S, a difference was observed in M1. No such differences between the sides were shown for group-E (Figure 3).

For **Ca**, the content is lower in group-E and group-S compared to group-C. At the same time, there is a difference between group-E and group-S. No differences were shown between individual molars (M1–3) (Figure 4).

The content of **Zn** was higher in group-E and group-S compared to group-C. At the same time, a difference was observed between group-E and group-S (Figure 5).

For **Sr**, the content is lower in group-E and group-S. At the same time, there is a difference between group-E and group-S (Figure 6).

## Discussion

We believe that the finding of a neurogenic effect on tooth tissue is important (Jacobsen and Heyeraas, 1996; Fristad, 1997; Byers et al., 2003; Berkovitz, 2016). We expected to observe substantial changes in element contents on the operated side in the study. However, as shown by the results, similar changes occur also on the opposite side of the mandible.

The subsiding of neuralgia after a surgery on the opposite side was documented by Kunc (1976). As found by this author, vertical nucleotomy affects also the contralateral second neuron, which, past the crossing point, runs not far from the hilum of the nucleus caudalis (Kunc, 1976). This fact explains our results (change in element contents on the contralateral side, as well) – although the IAN was transected only on one side, the contralateral nerve ending became affected, as well.

As follows from the study of Travers (2015), the spinal trigeminal nucleus affects afferentation of the ipsilateral trigeminal motor nucleus, and via connections from the reticular formation to the hypothalamus and up to the cerebral cortex it affects the contralateral region supplied by the trigeminal nerve. As follows from the above mentioned study, the transection of IAN causes changes in the spinal trigeminal nucleus and affects the other side of the mandible, as well.

These facts can have an impact on mastication of the animal and thus on mandibular load. As reported by various authors, the loading of the mandible affects bone mineralization, which is different in various parts of the mandible (Tanaka et al., 2007; de Jong et al., 2013; Hichijo et al., 2015).

We believe that these effects are involved in the change of element contents in the mandibular molars, and particularly, in concurrent changes of element contents on both sides of the mandible as shown in our study.

As reported by Jacobsen and Heyeraas (1996) in their study, the transection of IAN resulted in an almost complete loss of immunoreactive fibrils in the pulp and in a reduction of dentin production compared to the control group.

We did not show any statistically significant change in the weight of the animals during the 4-week observation period. We thus do not expect an effect of food intake on the contents of chemical elements in the molars.

Given that no description of effects of transectioning this nerve on chemical elements in teeth is found in available literature, it is difficult to perform any comparison to previous studies.

Statistically significant differences between the control and experimental groups and a difference between the experimental and sham groups support the concept that the transection of the nerve actually has an effect on the chemical elements. If no difference is found between the experimental and sham groups but a difference is found between both of these groups and the control group, such results indicate an effect of the surgery itself.

The transection of the nerve causes a reduction of the contents of the following elements in mandibular molars: Ca, and Sr. Additionally, an increase in the contents of Mg and Zn were caused. Furthermore, the transection caused a difference arrangement of both sides in Na.

The surgery caused a decrease in the contents of Na and K in the experimental and sham group. Furthermore, the difference in K in M3 between the left and right sides disappeared due to the surgery.

As reported by Naftel et al. (1999) in relation to the nerve supply of the molars in the rat, branches of the IAN innervate the M1 and anterior part of the M2. Distal part of the M2 and M3 innervate by branch of the lingual nerve.

The transection of the IAN caused a change in the inorganic component of the M1 and M2, but also of the M3. Our experience and literary date do not explain this fact.

## Conclusion

Our results have confirmed the hypothesis of IAN transection having an effect on the inorganic components in mandibular molars in the rat. This means that changes in mandibular molars in humans can be expected upon IAN transection, meaning that the nervous system is involved. Principal changes in the inorganic component of molars should be expected after an injury to IAN associated with maxillofacial surgery procedures, trauma or planned transection of the nerve in mandibular osteotomy or resection procedures. All consequences of these changes should thus be taken into account as regards the prognosis of individual molars in the mandible. We assume that a change of the mineralization of teeth can affect, for example, the occurrence of caries. As follows from our study, these changes involve molars on both sides of the mandible. Additionally, surgical approach to the nerve itself has an impact on mineralization of the teeth, as indicated by the study.

*Acknowledgements: The authors thank to Marie Fayadová (Institute of Geochemistry, Mineralogy and Mineral Resources, Faculty of Science, Charles University, Prague) for her help with mineralization of samples.*

## References

- Abd-Elmeguid, A., Yu, D. C. (2009) Dental pulp neurophysiology: Part 1. Clinical and diagnostic implications. *J. Can. Dent. Assoc.* **75**, 55–59.
- Abou Neel, E. A., Aljabo, A., Strange, A., Ibrahim, S., Coathup, M., Young, A. M., Bozec, L., Mudera, V. (2016) Demineralization-remineralization dynamics in teeth and bone. *Int. J. Nanomedicine* **11**, 4743–4763.
- Baxmann, M. (2006) Mental paresthesia and orthodontic treatment. *Angle Orthod.* **76**, 533–537.
- Berkovitz, B. K. B. (2016) Oral cavity. Chapter 31. In: *Gray's Anatomy: The Anatomical Basis of Clinical Practice*, Forty-first Edition, ed. Standing, S., pp. 507–533, Elsevier Limited, New York.
- Bhat, P., Cariappa, K. M. (2012) Inferior alveolar nerve deficits and recovery following surgical removal of impacted mandibular third molars. *J. Maxillofac. Oral Surg.* **11**, 304–308.
- Byers, M. R., Suzuki, H., Maeda, T. (2003) Dental neuroplasticity, neuro-pulpal interactions, and nerve regeneration. *Microsc. Res. Tech.* **60**, 503–515.
- Curzon, M. E. J., Crocker, D. C. (1978) Relationships of trace elements in human tooth enamel to dental caries. *Arch. Oral Biol.* **23**, 647–653.
- Curzon, M. E. J., Cutress, T. W. (1983) *Trace Elements and Dental Disease*. John Wright, PSG Inc., Boston.
- de Jong, W. C., van Ruijven, L. J., Brugman, P., Langenbach, G. E. (2013) Variation of the mineral density in cortical bone may serve to keep strain amplitudes within a physiological range. *Bone* **55**, 391–399.
- Dermience, M., Lognay, G., Mathieu, F., Goyens, P. (2015) Effects of thirty elements on bone metabolism. *J. Trace Elem. Med. Biol.* **32**, 86–106.
- Fischer, A., Wiechuła, D., Postek-Stefańska, L., Kwapiuliński, J. (2009) Concentrations of metals in maxilla and mandible deciduous and permanent human teeth. *Biol. Trace Elem. Res.* **132**, 19–26.
- Fischer, A., Wiechuła, D., Przybyła-Misztela, C. (2013) Changes of concentrations of elements in deciduous teeth with age. *Biol. Trace Elem. Res.* **154**, 427–432.
- Fristad, I. (1997) Dental innervation: Functions and plasticity after peripheral injury. *Acta Odontol. Scand.* **55**, 236–254.
- Ghadimi, E., Eimar, H., Marelli, B., Nazhat, S. N., Asgharian, M., Vali, H., Tamimi, F. (2013) Trace elements can influence the physical properties of tooth enamel. *Springerplus* **2**, 499.
- Hichijo, N., Tanaka, E., Kawai, N., van Ruijven, L. J., Langenbach, G. E. J. (2015) Effects of decreased occlusal loading during growth on the mandibular bone characteristics. *PLoS One* **10**, e0129290.
- Jacobsen, E. B., Heyeraas, K. J. (1996) Effect of capsaicin treatment or inferior alveolar nerve resection on dentine formation and calcitonin gene-related peptide- and substance P-immunoreactive nerve fibres in rat molar pulp. *Arch. Oral Biol.* **41**, 1121–1131.
- Kunc, Z. (1976) Bilateral trigeminal neuralgia. *Česk. Neurol. Neurochir.* **39**, 305–309.
- Lane, D. W., Peach, D. F. (1997) Some observations on the trace element concentrations in human dental enamel. *Biol. Trace Elem. Res.* **60**, 1–11.
- Meloun, M., Hill, M., Militký, J., Kupka, K. (2000) Transformation in the PC-aided biochemical data analysis. *Clin. Chem. Lab. Med.* **38**, 553–559.
- Meloun, M., Militký, J., Hill, M., Brereton, R. G. (2002) Crucial problems in regression modeling and their solutions. *Analyst* **127**, 433–450.
- Meloun, M., Hill, M., Militký, J., Vrbíková, J., Stanická, S., Škrha, J. (2004) New methodology of influential point detection in regression model building for the prediction of metabolic clearance rate of glucose. *Clin. Chem. Lab. Med.* **42**, 311–322.
- Naftel, J. P., Richards, L. P., Pan, M., Bernanke, J. M. (1999) Course and composition of the nerves that supply the mandibular teeth of the rat. *Anat. Rec.* **256**, 433–447.
- Němec, I., Smrčka, V., Pokorný, J. (2018a) The effect of sensory innervation on the inorganic component of bones and teeth; experimental denervation – Review. *Prague Med. Rep.* **119**, 137–147.

- Němec, I., Smrčka, V., Mihaljevič, M., Mazánek, J., Pokorný, J. (2018b) Multielemental chemical analysis of elements in mandibular bone and teeth in rat. *Folia Biol. (Praha)* **64**, 84–96.
- Ozkan, B. T., Celik, S., Durmus, E. (2008) Paresthesia of the mental nerve stem from periapical infection of mandibular canine tooth: a case report. *Oral Surg. Oral Med. Oral Pathol. Oral Radiol. Endod.* **105**, e28–e31.
- Reitznerová, E., Amarasiriwardena, D., Kopčáková, M., Barnes, R. M. (2000) Determination of some trace elements in human tooth enamel. *Fresenius J. Anal. Chem.* **367**, 748–754.
- Singh, R. K., Pal, U. S., Singh, P., Singh, G. (2016) Role of fixation in posttraumatic nerve injury recovery in displaced mandibular angle fracture. *Natl. J. Maxillofac. Surg.* **7**, 29–32.
- Tanaka, E., Sano, R., Kawai, N., Langenbach, G. E., Brugman, P., Tanne, K., van Eijden, T. M. (2007) Effect of food consistency on the degree of mineralization in the rat mandible. *Ann. Biomed. Eng.* **35**, 1617–1621.
- Travers, J. B. (2015) Oromotor nuclei. Chapter 11. In: *The Rat Nervous System*, Forth Edition, ed. Paxinos, G., pp. 223–245, Academic Press Elsevier, San Diego.
- Vrbič, V., Štupar, J., Byrne, A. R. (1987) Trace element content of primary and permanent tooth enamel. *Caries Res.* **21**, 37–39.
- Wilhelm, Z. (2007) Co je dobré vědět o vápníku. *Prakt. Lékáren.* **4**, 184–189.

# Endoscopic Resection of Upper Gastrointestinal Subepithelial Tumours: Our Clinical Experience and Results

**Mehmet Zeki Buldanlı<sup>1</sup>, Oktay Yener<sup>2</sup>**

<sup>1</sup>Department of General Surgery, University of Health Sciences, Gülhane Training and Research Hospital, Ankara, Turkey;

<sup>2</sup>Department of General Surgery, Istanbul Medeniyet University, Göztepe Training and Research Hospital, Istanbul, Turkey

Received February 3, 2021; Accepted January 31, 2022.

**Key words:** Endoscopy – Subepithelial tumour – Upper gastrointestinal diseases – Endoscopic submucosal dissection

**Abstract:** Upper gastrointestinal subepithelial tumours (SETs) are generally asymptomatic and clinically insignificant and have malign, borderline and benign variants. In advanced endoscopic procedures, histopathological diagnosis and endoscopic resection are possible and feasible. In this study, we examined our approach to upper gastrointestinal subepithelial tumours and our clinical results. Adult patients who applied to Surgical Endoscopy unit between January 2014 and January 2015 were included in the study. The patients' files and final histopathological diagnoses were recorded and analysed retrospectively for this single-center study. SET lesion lower than 30 mm and the lesion whose endoscopic submucosal dissection attemptation was included in the study. The total of 8 patients were four female (50%) and four male (50%), aged 31–66 years (median, 53 years). The tumoral lesions were located 4 (50%) patients in esophagus, 3 (37.5%) patients in stomach and one (12.5%) patient in duodenum and their diameter ranged from 5 to 30 mm (median, 14 mm). Post-interventional no complications or abdominal symptoms were encountered. Also, in early follow-ups for six months, no recurrence was observed. Our experiences together with literature reported here, indicated endoscopic resection is a safe and effective method of treatment for most patients with upper gastrointestinal SETs.

**Mailing Address:** Dr. Oktay Yener, Department of General Surgery, Istanbul Medeniyet University, Göztepe Training and Research Hospital, Plaj Yolu Kaya apt. 23/10, Caddebostan, Istanbul, Turkey; e-mail [oktayener@gmail.com](mailto:oktayener@gmail.com)

## Introduction

Submucosal masses or lesions often referred to as “submucosal tumours”, represent a growth underneath the mucosa of the gastrointestinal (GI) tract whose etiology cannot be determined by GI endoscopy or barium contrast studies (Geis et al., 1996). It can also be detected with oral contrast-enhanced abdominal computed tomography (CT). However, the term “submucosal tumour” is inappropriate, because many of these lesions do not arise from the submucosa and many of them are not tumours (Halpin et al., 1993). Thus, “subepithelial” is a more appropriate term than “submucosal”. Hence, other authors call these abnormalities subepithelial lesions, because they are covered by normal mucosa. These can be caused by external compression by the neighbouring organs or by intramural lesions. However, submucosal is still recognized and used (Kojima et al., 1999; Sakamoto et al., 2010).

Upper GI subepithelial tumours (SETs) are generally asymptomatic and clinically insignificant and have malign, borderline and benign variants with various histopathological types. In advanced upper GI endoscopic procedures, histopathological diagnosis and endoscopic resection are possible and feasible (Cho and Korean ESD Study Group, 2016). In this study, we examined our approach to upper gastrointestinal subepithelial tumours and our clinical results.

## Material and Methods

Adult patients who applied to Istanbul Medeniyet University, Göztepe Training and Research Hospital, Department of General Surgery, Surgical Endoscopy unit between January 2014 and January 2015 were included in the study. The patients' files and final histopathological reports including diagnoses were recorded and analysed retrospectively for this single-center study. SET lesion lower than 30 mm and the lesion whose endoscopic submucosal dissection (ESD) attempt was included in the study.

Upper GI endoscopy was planned for the patients with appropriate indications in line with their upper gastrointestinal system complaints. The procedure was planned after oral and intravenous contrast-enhanced abdominal CT. Submucosal lesion of the stomach was found by upper gastrointestinal endoscopy performed. Complete blood count (CBC), coagulation and routine biochemistry blood tests were performed in all patients before the procedure. All patients were referred for pre-interventional anesthesia examination. Acetyl salicylic acid and/or other anticoagulant drugs were withdrawn before intervention. Patients informed consent was taken before endoscopic procedures. After 8 hours of fasting, the procedures were performed by the same endoscopy team in a single center. Surgeon as an endoscopist, endoscopy technician, surgery resident, anesthesiologist and anesthesia technician participated in the procedures. Vital signs of the patients were monitored during the procedure. Sedation was performed with topical anesthetic drugs and intravenous propofol and managed by the anesthesiologist.

The procedure was started with standard gastroscope after the sedation. Gastric residuals were cleaned by gastric irrigation and aspiration with 0.9% normal saline solution for proper visualization and also detecting the lesion with margins. Endoscopic submucosal dissection was carried out as follows; special solution (0.4% hyaluronic acid, 2 ml indigo carmine, 1/10.000 epinephrine, 0.9% normal saline solution) was injected by endoscopic injector into the submucosal layer for lifting the lesion at the marked margin of resection, moving from a distal to a proximal direction, and the lesion was elevated. Circumferential incision was performed by endoscopic knife and endoscopic cautery for the *en bloc* excision from surrounding tissue. The submucosal lesion was dissected using an endoscopic snare and an endoscopic cutting knife. Then the tumour was resected from the surrounding tissues with negative surgical margins. If needed, endoscopic cautery and/or clips were used for hemostasis after resection. The specimen was extracted by endoscopic snare or endoscopic grasper and sent to the medical pathology department for histopathological examination.

If there was any concern about the complications (bleeding, perforation or anesthetic complications) post-procedurally, the patients were hospitalized and followed-up closely.

This study complied with the World Medical Association Declaration of Helsinki. Statistically, median and percentage values calculated with Microsoft Office Excel® program.

## Results

The total of 8 patients were four female (50%) and four male (50%), aged 31–66 years (median, 53 years). The tumoral lesions were located 4 (50%) patients in the distal esophagus, 3 (37.5%) patients in fundus part of stomach and one (12.5%) patient in bulbus duodeni and their diameter ranged from 5 to 30 mm (median, 14 mm) (Table 1). They were diagnosed as SETs from the upper GI endoscopic appearance. Final histopathological diagnoses were benign leiomyoma in 5 (62.5%) patients (Figure 1). The other diagnoses were gastrointestinal mesenchymal tumour, lipoma and gastrointestinal stromal tumour (GIST) (Table 1). When histopathological evaluation is made according to localization; three leiomyomas were in distal esophagus and two leiomyomas were in stomach. Also, one GIST was in stomach, one lipoma was in distal esophagus and one gastrointestinal mesenchymal tumour was in bulbus duodeni. When the pathology reports were examined, it was determined that all specimens were resected as the R0 resection and surgical margins were clear.

Leiomyomas were detected microscopically as smooth muscle tumour with minimal atypia and stained positively by smooth muscle actin and desmin. GIST was detected as sclerosing spindle subtype with bland spindle cells and stained positively c-KIT (CD117) and DOG-1. Lipoma was detected as mature homogeneous adipose tissue without atypia. Gastrointestinal mesenchymal tumour detected as an

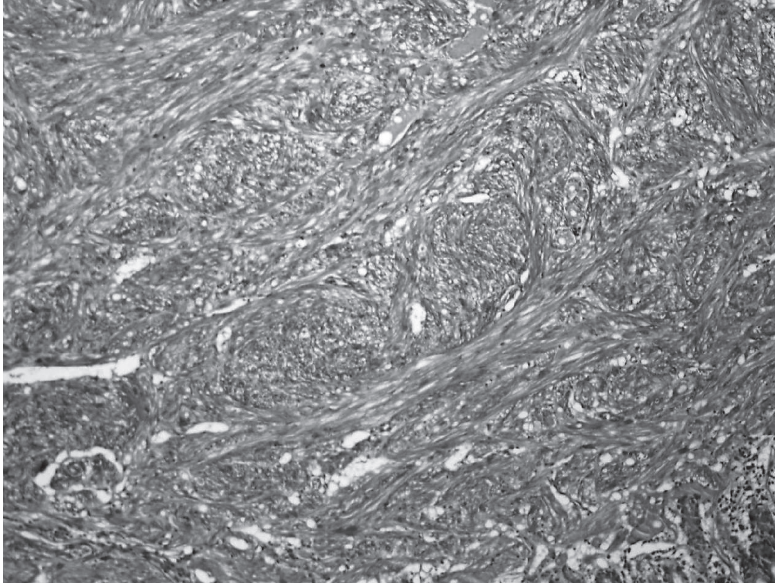


Figure 1 – Histological appearance of the benign subepithelial lesion (stained with hematoxylin-eosin,  $\times 10$ ).

**Table 1 – Demographic and tumour characteristics of patients**

Age (year)	31–66 (53)
Gender, male/female, n (%)	4/4 (50%/50%)
Tumour size (mm)	5–30 (14)
Tumour localization, n (%)	
Esophagus	4 (50.0%)
Stomach	3 (37.5%)
Duodenum	1 (12.5%)
Final histopathological diagnosis of tumour, n (%)	
Leiomyom	5 (62.5%)
GIST	1 (12.5%)
Gastrointestinal mesenchymal tumour	1 (12.5%)
Lipoma	1 (12.5%)

Values are median or n (%); GIST – gastrointestinal stromal tumour

inflammatory myofibroblastic tumour with myofibroblastic spindle cell proliferation and mixed inflammation microscopically. It was stained by vimentin and ALK-1 positively.

Post-interventional no complications or abdominal symptoms were encountered. After the procedure, the patients were informed in detail about the process. Oral

intake was started in four hour later without any trouble. If there was a concern about complications oral intake delayed. Patients were discharged with oral proton pump inhibitor and sucralfate medical treatment, recommendations and follow-up planning. The first control examination was scheduled for 15 days. In this way, patients were also informed about their histopathological findings. Subsequent follow-up examinations were scheduled at the first month, third month, and sixth month. In the third and sixth months, endoscopic evaluation controls were also performed, no pathology was observed. By the way, in follow-ups for six months, no recurrence or complications were observed.

## Discussion

The majority of subepithelial tumours do not cause symptoms and are discovered incidentally during endoscopic or radiologic examinations. The overlying mucosa usually appears smooth and normal at endoscopy. If symptoms do occur, they are nonspecific such as abdominal pain, obstruction, hemorrhage and intussusceptions (Sakamoto et al., 2010; Inoue et al., 2012). Large submucosal neoplasms may outgrow their blood supply, ulcerate through the mucosa, and present as GI bleeding. Firm subepithelial tumours may also present with obstructive symptoms, especially if they are located near the cardia or the pylorus. Subepithelial tumours obstructing the major or minor papilla may cause jaundice or pancreatitis. Pain and weight loss, often associated with large submucosal GISTs, are symptoms that suggest malignancy (Iwahashi et al., 2006). In this study, our patients presented with dyspeptic complaints and upper abdominal pain.

Park et al. (2004) have recently reported the experience of endoscopic enucleation of submucosal tumours of the esophagus and the stomach in 15 patients. There were four patients with GISTs of the stomach. Tumour tissue was removed completely in these patients but a small perforation occurred in one patient, in whom the tumour involved the muscularis propria and had grown outward to the serosa. In this study, the esophageal and gastric procedure performed to seven patients and no early complications were observed in these patients.

Rosch et al. (2004) have treated 14 patients with submucosal tumours of the esophagus and the stomach by endoscopic surgery. In their series, there were five patients with GIST of the stomach. No serious complications were encountered in these patients but complete removal was uncertain in two patients with gastric GISTs that originated in the muscularis propria. In this study, no complications or early recurrence were observed after the procedure. Also, all specimens were resected as the R0 resection and surgical margins were clear.

In a series of 51 patients by Chiu et al. (2019), the importance of location and size for the SET intervention was emphasized. Especially, per oral endoscopic tumour resection (POAT) was found safe for esophageal and gastric SET located at cardia, lesser curvature, and antrum. Also, they limited the tumour size < 40 mm. In this study, tumour localizations and sizes are similar. POAT as an advanced minimal

invasive technique, was not experienced in our center. So, we could not perform this procedure on patients with similar characteristics.

Endoscopic ultrasonography (EUS) can give findings in the differential diagnosis of SETs and in determining which tunica layer originates from. In addition, histopathological sampling can be done before the procedure with endoscopic ultrasound-guided fine needle aspiration and biopsy. For this reason, it can be considered in experienced centers together with interventional endoscopic procedures (Kim et al., 2019). In this study, CT imaging and routine endoscopy were performed pre-interventional and the patients were informed about not performing EUS and their consent was obtained.

With the development of endoscopic techniques and minimal invasive procedures, surgical procedures for intervention in SETs leave their place to endoscopic interventions. Endoscopic submucosal dissection (ESD), endoscopic enucleation, endoscopic excavation, endoscopic submucosal tunnel dissection, submucosal tunnel endoscopic resection, and endoscopic full-thickness resection (EFTR) are options for this treatment. Also, after these procedures endoscopic clipping can be performed because of the risk for bleeding (Kim and Kim, 2018). In this study, routine ESD procedure was applied after lifting and no problems were encountered during the procedure.

Kim et al. (2011) reported that the major complications of the ESD are bleeding and perforation. Perforation was stated with a rate of 4% in the first studies about this topic, but it is stated that this rate is decreasing with increasing experience. Bleeding was obtained with rates from 13 to 38%. Stenosis, transient bacteremia, aspiration pneumonia, thromboembolism and anesthetic complications are other complications that were specified in the literature (Saito et al., 2014). In this study, per-interventional minor bleedings were encountered and immediate successful hemostasis performed with the endoscopic cautery and/or clips. Perforation and other complications were not observed.

In the literature, it was observed that follow-up was ranged from 6.1 months to 19.1 months after endoscopic procedures. These follow-ups were made with endoscopy and examinations. No recurrence was observed among the patients with complete resection in included studies (Kim and Kim, 2016). In this study, the patients were followed-up for six months and recurrence was not observed as well.

The limitations of this study are the low number of patients, not performing of other advanced endoscopic interventions and procedures for this study, the short post-interventional follow-up period with results and retrospective design of study.

## **Conclusion**

Consequently, our experiences together with literature reported here, indicated endoscopic resection is a safe and effective method of treatment for most patients with upper gastrointestinal SETs. However, prospective randomized studies and reviews involving more patient populations are needed for this subject.

## References

- Chiu, P. W. Y., Yip, H. C., Teoh, A. Y. B., Wong, V. W. Y., Chan, S. M., Wong, S. K. H., Ng, E. K. W. (2019) Per oral endoscopic tumor (POET) resection for treatment of upper gastrointestinal subepithelial tumors. *Surg. Endosc.* **33(4)**, 1326–1333.
- Cho, J. W., Korean ESD Study Group (2016) Current guidelines in the management of upper gastrointestinal subepithelial tumors. *Clin. Endosc.* **49(3)**, 235–240.
- Geis, W., Baxt, R., Kim, H. C. (1996) Benign gastric tumors. Minimally invasive approach. *Surg. Endosc.* **10(4)**, 407–410.
- Halpin, R., Thomson, S., Catterall, N., Haffejee, A. (1993) Smooth muscle tumors of the stomach: Clinicopathological aspects. *J. R. Coll. Surg. Edinb.* **38(1)**, 23–27.
- Inoue, H., Ikeda, H., Hosoya, T., Onimaru, M., Yoshida, A., Eleftheriadis, N., Maselli, R., Kudo, S. (2012) Submucosal endoscopic tumor resection for subepithelial tumors in the esophagus and cardia. *Endoscopy* **44(3)**, 225–230.
- Iwahashi, M., Takifuji, K., Ojima, T., Nakamura, M., Nakamori, M., Nakatani, Y., Ueda, K., Ishida, K., Naka, T., Ono, K., Yamaue, H. (2006) Surgical management of small gastrointestinal stromal tumors of the stomach. *World J. Surg.* **30(1)**, 28–35.
- Kim, S. G., Song, J. H., Hwang, J. H. (2019) Current status of endoscopic ultrasonography in gastrointestinal subepithelial tumors. *Clin. Endosc.* **52(4)**, 301–305.
- Kim, S. H., Moon, J. S., Youn, Y. H., Lee, K. M., Lee, S. J. (2011) Management of the complications of endoscopic submucosal dissection. *World J. Gastroenterol.* **17(31)**, 3575–3579.
- Kim, S. Y., Kim, K. O. (2016) Management of gastric subepithelial tumors: The role of endoscopy. *World J. Gastrointest. Endosc.* **8(11)**, 418–424.
- Kim, S. Y., Kim, K. O. (2018) Endoscopic treatment of subepithelial tumors. *Clin. Endosc.* **51(1)**, 19–27.
- Kojima, T., Takahashi, H., Parra-Blanco, A., Kohsen, K., Fujita, R. (1999) Diagnosis of submucosal tumor of the upper GI tract by endoscopic resection. *Gastrointest. Endosc.* **50(4)**, 516–522.
- Park, Y. S., Park, S. W., Kim, T. I., Song, S. Y., Choi, E. H., Chung, J. B., Kang, J. K. (2004) Endoscopic enucleation of upper-GI submucosal tumors by using an insulated-tip electrosurgical knife. *Gastrointest. Endosc.* **59(3)**, 409–415.
- Rosch, T., Sarbia, M., Schumacher, B., Deinert, K., Frimberger, E., Toerner, T., Stolte, M., Neuhaus, H. (2004) Attempted endoscopic en bloc resection of mucosal and submucosal tumors using insulated-tip knives: a pilot series. *Endoscopy* **36(9)**, 788–801.
- Saito, I., Tsuji, Y., Sakaguchi, Y., Niimi, K., Ono, S., Kodashima, S., Yamamichi, N., Fujishiro, M., Koike, K. (2014) Complications related to gastric endoscopic submucosal dissection and their managements. *Clin. Endosc.* **47(5)**, 398–403.
- Sakamoto, H., Kitano, M., Kudo, M. (2010) Diagnosis of subepithelial tumors in the upper gastrointestinal tract by endoscopic ultrasonography. *World J. Radiol.* **2(8)**, 289–297.

# POEMS Syndrome Diagnosis in a Patient with Mixed Polyneuropathy: Case Report

**Maria Isabel Ocampo-Navia<sup>1</sup>, María Andrea Negret Noreña<sup>2</sup>, Luis Rafael Chaparro Santos<sup>3</sup>, José Ricardo Morera Afanador<sup>3</sup>, Ricardo Andrés Quintero Farías<sup>3</sup>, José Luis Bustos Sánchez<sup>4</sup>**

<sup>1</sup>Department of Neurosurgery, Hospital Universitario San Ignacio, Pontificia Universidad Javeriana, Bogotá, Colombia;

<sup>2</sup>Department of Internal Medicine, Hospital Universitario San Ignacio, Pontificia Universidad Javeriana, Bogotá, Colombia;

<sup>3</sup>Department of Internal Medicine, Hospital Universitario San Rafael de Tunja, Boyacá, Colombia;

<sup>4</sup>Department of Neuroscience, Hospital Universitario San Rafael de Tunja, Boyacá, Colombia

Received July 30, 2020; Accepted February 16, 2022.

**Key words:** Paraproteinemia – POEMS syndrome – Plasma cells – Plasmocytoma – Polyneuropathy

**Abstract:** POEMS syndrome is a rare condition of paraneoplastic origin characterized by the presence of a sensorimotor polyneuropathy associated with the presence of a proliferative disorder of plasmatic monoclonal cells and overproduction of vascular endothelial growth factor. The acronym “POEMS” represents multisystem findings including polyneuropathy, organomegaly, endocrinopathy, monoclonal plasma cell disorder and skin changes; nevertheless, clinical presentation is heterogeneous. We describe a clinical case, the diagnostic and therapeutic approach in a patient with sensorimotor polyneuropathy in whom POEMS syndrome was diagnosed; to understand this pathology, its clinical and paraclinical manifestations in order to make a diagnosis or to avoid a delayed one and to provide an adequate treatment.

**Mailing Address:** Maria Isabel Ocampo-Navia, MD., Department of Neurosurgery, Pontificia Universidad Javeriana, Cra. 7#40-62, 6<sup>th</sup> floor, Bogotá 111017, Colombia; e-mail: maria\_ocampo@javeriana.edu.co

<https://doi.org/10.14712/23362936.2022.3>

© 2022 The Authors. This is an open-access article distributed under the terms of the Creative Commons Attribution License (<http://creativecommons.org/licenses/by/4.0>).

## Introduction

POEMS syndrome (Polyneuropathy, Organomegaly, Endocrinopathy, Monoclonal protein, Skin changes) is a rare disease, usually related to a paraneoplastic etiology, characterized by the presence of a monoclonal plasma cell disorder, peripheral neuropathy, and increased levels of serum vascular endothelial growth factor (VEGF) (Plaza et al., 2016; Keddie et al., 2018). The acronym “POEMS” references the most frequent symptoms including: **P**olyneuropathy, **O**rganomegaly, **E**ndocrinopathy, **M**onoclonal protein, and specific **S**kin changes (Plaza et al., 2016; Keddie et al., 2018). Nonetheless, clinical presentation varies greatly in each individual case, and may not present all the criteria. Suichi et al. (2019) estimated a prevalence of 0.3 for 100,000 people, however due to the rarity of said entity, this usually implies a delayed, or even subdiagnosis.

Given that POEMS syndrome is an incapacitating condition, related to high morbidity if not treated early, an opportune diagnosis is key to a more favourable prognosis and adequate lifestyle for these patients. More aggressive treatment options have been used since 2000, including high doses of chemotherapy along with autologous stem cell transplant, immunomodulators, and proteasome inhibitors (Kuwabara et al., 2012; Dispenzieri, 2017; Suichi et al., 2019). The latest evidence establishes that monoclonal antibodies against VEGF are harmful and can lead to death. This suggests that although a useful biomarker in the diagnostic stage, VEGFs pathophysiological role is poorly understood.

This syndrome is unfortunately rarely considered as a differential diagnosis among patients presenting with chronic polyneuropathy without any other related symptoms due to a generalized insufficient knowledge about said condition. This is why a better diagnostic approach plays a fundamental role in avoiding unnecessary studies and can lead to an early diagnostic approach. The objective of this article is to describe a clinical case, along with its diagnostic and therapeutic process, in a patient with mixed polyneuropathy ultimately diagnosed with POEMS syndrome.

## Case report

A 47-year-old man, with a history of acute myocardial infarction with reduced left ventricular ejection fraction, who presents with 6 months of progressive distal muscle weakness that limits functionality, along with paresthesias in all four extremities, and significant weight loss. During the physical examination, generalized areflexia and hypertrophy of both lower limbs are evident.

The electromyography and nerve conduction showed a severe, predominantly demyelinating, polyneuropathy that affected both the motor and sensitive nerves in all four extremities, with a few signs of active denervation.

Other etiologies were ruled out, including deficiencies, metabolic causes, autoimmune and paraneoplastic causes (Table 1). A tomographic search for neoplastic lesions concluded mild diffuse hepatosplenomegaly and ascites. The

**Table 1 – Patient laboratory results**

	<b>Laboratory tests</b>	<b>Value</b>
Blood chemistry panel	hemoglobine	10 g/dl
	hematocrite	30%
	leucocytes	11,000
	platelets	332,000
	glucose	88 mg/dl
Endocrine tests	TSH	3.15 mUI/l (0.27–4.2)
	cortisol AM	10 ug/dl (100–140 mmol/l)
	ACTH	515 pg/ml (6–76 pg/ml)
Metabolic tests	proteins	6 g/dl
	albumin	3 g/dl
	B12 vitamine	653 pg/ml
	folic acid	15 ng/ml
Autoimmune tests	ANAS	1:80 diluciones
	pANCAS and cANCAS	negative
	ENAS (Ro, Sm, La, Rnp)	negative
	lupus anticoagulant	negative

TSH – thyroid-stimulating hormone; ACTH – adrenocorticotrophic hormone

patient was sent home with an unsure diagnosis of a chronic, inflammatory demyelinating polyneuropathy to be treated with corticoids.

Ten months later, the patient returns with worsening paraparesis and dysesthesias, along with an exacerbation of his neurological deficit over the last 20 days, accompanied by edema of both legs (Figure 1). During the physical examination, the patient presents unresponsive hypotension, jugular engorgement, leukonychia, ascites and pitting edema of the lower limbs. Neurological findings include hypotrophy of all four extremities, strength 3/5 in upper limbs and 2/5 in lower limbs, generalized areflexia and distal multimodal hypoesthesia in lower limbs.

Considering a possible chronic polyneuropathy of unknown origin with unclear multisystemic findings, further studies were required. Due to sustained hypotension in spite of vasopressors, endocrine tests were performed which confirmed adrenal insufficiency secondary to low cortisol levels and high ACTH (adrenocorticotrophic hormone) levels (Table 1). A new thoracoabdominal computed tomography (CT) showed increased hepatosplenomegaly (Figure 1).

A lumbar puncture reported an albumin-cytological dissociation which led to a sural nerve biopsy that ultimately reported an inflammatory demyelinating mixed axonal neuropathy, in addition to a serum protein electrophoresis that showed slightly elevated levels of beta-1, beta-2, and gamma. Given these findings, serum immunofixation was done which showed IgA lambda monoclonal gammopathy.

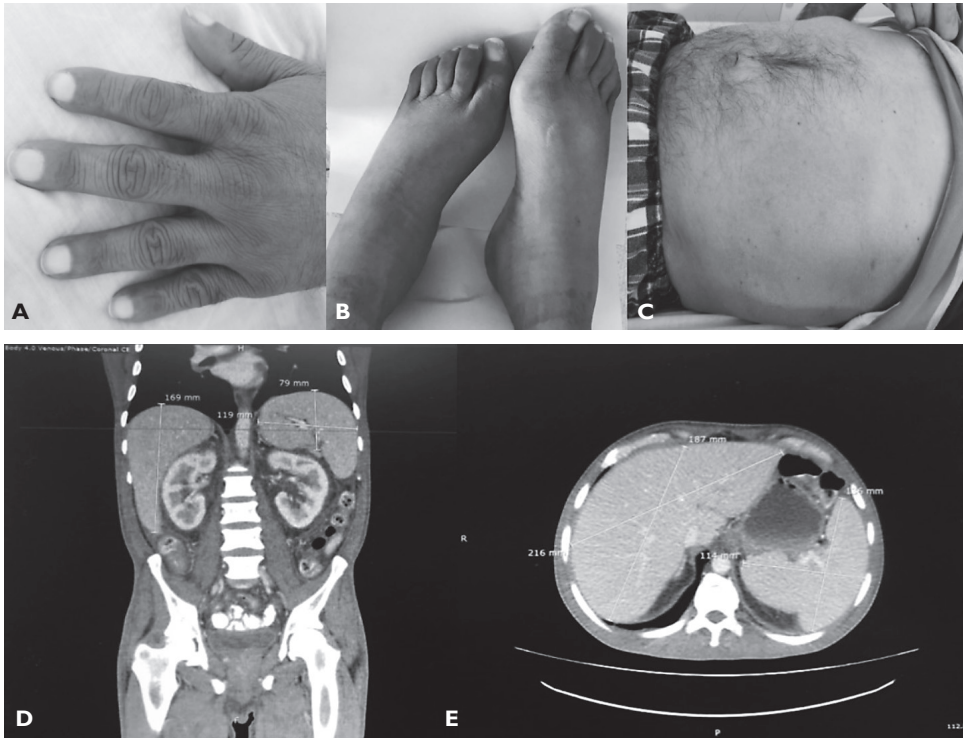


Figure 1 – Semiologic findings of the patient compatible with POEMS syndrome. A) leukonychia; B) edema; C) ascites; D) and E) hepatosplenomegaly.

Everything described previously led to a bone marrow biopsy which resulted in megakaryocytic hyperplasia, dysmegakaryopoietic changes, and increased plasmacytes.

POEMS syndrome became a more likely diagnostic possibility once two major criteria and four minor criteria (organomegaly, endocrinopathy, skin changes and volume overload) were met. Therefore, long bone X-rays were taken which ruled out the presence of lithic or sclerotic lesions. Finally, the diagnosis was confirmed thanks to a VEGF of 433.9 pg/ml (normal: 128.9 pg/ml). The patient was then referred to a level of greater complexity for a hematology consult and to decide on an autologous hematopoietic cell transplant.

## Discussion

POEMS syndrome is a proliferative monoclonal plasma cell disorder that leads to a systemic inflammatory response mediated by the presence of cytokines (Gherardi et al., 1996; Michizono et al., 2001). VEGF is an angiogenic cytokine that is found significantly elevated in these cases, and therefore it is a strategic biomarker when

**Table 2 – Diagnostic criteria for POEMS syndrome**

Mandatory major criteria (both)	Polyneuropathy Monoclonal plasma cell-proliferative disorder
Major criteria (at least one)	Castleman's disease Sclerotic or lytic bone lesions Vascular endothelial growth factor elevation
Minor criteria (at least one)	Organomegaly (splenomegaly, hepatomegaly, or lymphadenopathy) Extravascular volume overload (edema, pleural effusions, or ascites) Endocrinopathy (adrenal, thyroid, pituitary, gonadal, parathyroid or pancreatic) Changes in skin: hypertrichosis, acrocyanosis, leukonychia Papilledema Thrombocytosis, polycythemia

making this diagnosis and during the follow-up (Watanabe et al., 1996; D'Souza et al., 2011; Keddie et al., 2018). However, the proper, official diagnosis is made using the criteria established by Dispenzieri et al. in 2003 that include clinical, paraclinical and imaging findings (Table 2).

The characteristic plasma cell disorder includes the presence monoclonal proteins, also known as paraproteins, in plasma, serum and/or urine. These are composed from a single heavy chain (M, G or A) and a single light chain (kappa or lambda). According to Vallat et al. (1996), the paraproteins usually associated to polyneuropathies tend to be IgM and kappa, which varies from a key aspect of POEMS, given that the latter tends to be associated to IgA or IgG and lambda light chains in 95% of cases, including the above-mentioned case (Vallat et al., 1996; Dispenzieri et al., 2003). In order to achieve a better test sensitivity, these proteins should be found through protein electrophoresis, immunofixation, and light chain analysis in both serum and urine samples. This should be taken in account, given that if only protein electrophoresis is done, there can be up to 30% false negatives (Dispenzieri et al., 2003).

Once confirmed, a bone marrow biopsy should be done in order to properly guide treatment. Approximately 66% of POEMS syndrome patients' biopsies will show a malignant cellular clone with a high rate of cellular abnormalities limited to expressing lambda light chains (Dispenzieri et al., 2003; Dao et al., 2011; Keddie et al., 2018). The 33% of remaining biopsies that do not show these clones could point to a cellular disorder limited to solitary or multifocal plasmacytomas located in soft or bone tissues (Dao et al., 2011; Keddie et al., 2018). It should be noted that although in the case described no malignant clones or plasmacytomas were found in the bone marrow sample, their presence cannot be completely ruled out due to their extremely small size.

**Table 3 – POEMS syndrome diagnostic approach**

Characteristic	Diagnostic study	Typical abnormality
Polyneuropathy	Nerve conduction/ electromyography	Axonal and demyelinating polyneuropathy, more frequent demyelinating
	Nerve biopsy	Not necessary if diagnosis is clear with elevated VEGF levels. Axonal degeneration, diffuse myelinated fiber loss, increased epineural blood vessels
	Cerebrospinal fluid*	Albuminocytologic dissociation; normal cell count; mild increase opening pressure; not specific so not always necessary
Organomegaly	CT scan of chest/abdomen/ pelvis and PET-CT	Lymph node, spleen, liver
Endocrinopathy	Adrenal: cortisol	Typically low
	Thyroid: TSH, T4	Hypothyroid or hyperthyroid
	Pituitary: LH, FSH, IGF-1, ACTH, prolactin	Typically hypofunctioning
	Gonadal: testosterone, oestradiol	Typically low
	Parathyroid: PTH	
Monoclonal plasma cell disorder	Pancreatic: HbA1c, glucose	Typically raised
	Serum protein electrophoresis Immunofixation Serum free light chain analysis	IgG or IgA lambda monoclonal protein
	Urine protein electrophoresis/ immunofixation	Bence Jones proteins
Skin	Bone marrow biopsy ± targeted bone lesion biopsy	Presence of plasma cells in immunofixation, typically lambda light chain restricted
	Clinical diagnosis	Acrocyanosis, hypertrichosis, nail changes, glomerular hemangiomas
Papilledema	Ophthalmological assessment	
Extravascular volume overload/cardiac involvement	Echocardiogram*	Reduction of left or right ventricular ejection fraction, elevation of pulmonary artery pressure; evidence of previous ischemia
Sclerotic bone lesions	CT bone windows, PET-CT imaging	Sclerotic lesions/mixed lytic with sclerotic
Thrombocytosis	Full blood count	Increased platelets
Pulmonary function	Pulmonary function tests*	Pulmonary hypertension, restrictive disease, respiratory muscle weakness, reduced diffusion capacity

\*not necessary for diagnosis, but useful; VEGF – vascular endothelial growth factor; CT – computed tomography; PET – positron emission tomography; TSH – thyroid-stimulating hormone; ACTH – adrenocorticotropic hormone; LH – luteinizing hormone; PTH – parathyroid hormone; IGF-1 – insulin like growth factor-1

Due to the aforementioned, a CT or a positron emission tomography to assess the presence of lytic or bone sclerotic lesions should be taken. This is key, taking into account that a normal bone marrow biopsy could false lead to a missed or delayed diagnosis.

In what relates to the multisystemic findings, the endocrinopathy usually presents in around 65% of cases, more frequently as erectile dysfunction and gynecomastia in men, and as early menopause symptoms in women. Taking that into consideration, it is very interesting that our case presents an endocrinopathy as the adrenal insufficiency, which is a rarer disease. In regards to the organomegaly, only 50% of patients express it, and usually affecting the liver, spleen or lymphatics, as reflected in our patient's CT (Keddie et al., 2018). Lastly, multiple skin lesions have been described as frequent expression of POEMS including glomeruloid-like hemangiomas, reddish dome-shaped papules on the trunk and extremities, leukonychia and hypertrichosis (Keddie et al., 2018).

Though rare, it is a diagnosis that should be considered in patients with chronic, usually demyelinating, polyneuropathy of unclear origin who also present multisystemic findings. One of its main differential diagnosis is Demyelinating Chronic Inflammatory Polyneuropathy. Up to 60% of POEMS patients are initially diagnosed with said pathology, wrongly treated with immunomodulatory therapy, which would result ineffective and essentially just delay the actual diagnosis for a period of around 12 months (Nasu et al., 2012). Table 3 exhibits the diagnostic tools for a proper approach to POEMS syndrome.

As far as for treatment for POEMS, the use of monoclonal antibodies that block VEGF has been proved to be harmful to the patient, even fatal, which just goes to show that although a useful diagnostic biomarker, VEGF's pathophysiological role is still unclear (Keddie et al., 2018). The main therapeutic goal is to suppress monoclonal plasma cell proliferation. In cases with systemic affection (bone marrow, or 3 or more plasmacytomas), gold standard treatment includes autologous stem cell transplant and chemotherapy. In patients with localized affection (less than 2 plasmacytomas without bone marrow affection) radiotherapy is recommended (Dispenzieri, 2017; Keddie et al., 2018).

We depicted a clinical case describing a patient with POEMS syndrome, which was diagnosed taking into account the expression of multisystemic findings along with his chronic neuropathy. This report highlights the significance of an adequate semiological evaluation and high diagnostic suspicion to achieve a timely detection of this pathology, looking to avoid clinical progression and unnecessary studies. In closing, opportune treatment plays a fundamental role in avoiding clinical deterioration, therefore emphasizing the importance of considering POEMS syndrome a differential diagnosis in patients presenting with chronic polyneuropathy and Demyelinating Chronic Inflammatory Polyneuropathy accompanied by other seemingly unrelated findings.

## References

- D'Souza, A., Hayman, S. R., Buadi, F., Mauermann, M., Lacy, M. Q., Gertz, M. A., Kyle, R. A., Kumar, S., Greipp, P. R., Lust, J. A., Zeldenrust, S., Witzig, T. E., Raikumar, S. V., Dispenzieri, A. (2011) The utility of plasma vascular endothelial growth factor levels in the diagnosis and follow-up of patients with POEMS syndrome. *Blood* **118(17)**, 4663–4665.
- Dao, L. N., Hanson, C. A., Dispenzieri, A., Morice, W. G., Kurtin, P. J., Hoyer, J. D. (2011) Bone marrow histopathology in POEMS syndrome: A distinctive combination of plasma cell, lymphoid, and myeloid findings in 87 patients. *Blood* **117(24)**, 6438–6444.
- Dispenzieri, A. (2017) POEMS syndrome: 2017 update on diagnosis, risk stratification, and management. *Am. J. Hematol.* **92(8)**, 814–829.
- Dispenzieri, A., Kyle, R. A., Lacy, M. Q., Rajkumar, S. V., Therneau, T. M., Larson, D. R., Greipp, P. R., Witzig, T. E., Basu, R., Suarez, G. A., Fonseca, R., Lust, J. A., Gertz, M. A. (2003) POEMS syndrome: Definitions and long-term outcome. *Blood* **101(7)**, 2496–2506.
- Gherardi, R. K., Bélec, L., Soubrier, M., Malapert, D., Zuber, M., Viard, J. P., Intrator, L., Degos, J. D., Authier, F. J. (1996) Overproduction of proinflammatory cytokines imbalanced by their antagonists in POEMS syndrome. *Blood* **87(4)**, 1458–1465.
- Keddie, S., D'sa, S., Folds, D., Carr, A. S., Reilly, M. M., Lunn, M. P. T. (2018) POEMS neuropathy: Optimising diagnosis and management. *Pract. Neurol.* **18(4)**, 278–290.
- Kuwabara, S., Dispenzieri, A., Arimura, K., Misawa, S., Nakaseko, C. (2012) Treatment for POEMS (polyneuropathy, organomegaly, endocrinopathy, M-protein, and skin changes) syndrome. *Cochrane Database Syst. Rev.* **2012(6)**, CD006828.
- Michizono, K., Umehara, F., Hashiguchi, T., Arimura, K., Matsuura, E., Watanabe, O., Fujimoto, N., Okada, Y., Osame, M. (2001) Circulating levels of MMP-1, -2, -3, -9, and TIMP-1 are increased in POEMS syndrome. *Neurology* **56(6)**, 807–810.
- Nasu, S., Misawa, S., Sekiguchi, Y., Shibuya, K., Kanai, K., Fujimaki, Y., Ohmori, S., Mitsuma, S., Koga, S., Kuwabara, S. (2012) Different neurological and physiological profiles in POEMS syndrome and chronic inflammatory demyelinating polyneuropathy. *J. Neurol. Neurosurg. Psychiatry* **83(5)**, 476–479.
- Plaza, C., Arquer, R., García-Raso, A., Llamas, P. (2016) Diagnóstico de síndrome de POEMS tras neuropatía de larga evolución. *Neurología (Barcelona, Spain)* **34(4)**, 272–274.
- Suichi, T., Misawa, S., Beppu, M., Takahashi, S. (2019) Prevalence, clinical profiles, and prognosis of POEMS syndrome in Japanese nationwide survey. *Neurology* **93(10)**, 975–984.
- Vallat, J. M., Jauberteau, M. O., Bordessoule, D., Yardin, C., Preux, P. M., Couratier, P. (1996) Link between peripheral neuropathy and monoclonal dysglobulinemia: A study of 66 cases. *J. Neurol. Sci.* **137(2)**, 124–130.
- Watanabe, O., Arimura, K., Kitajima, I., Osame, M., Maruyama, I. (1996) Greatly raised vascular endothelial growth factor (VEGF) in POEMS syndrome. *Lancet* **347(9002)**, 702.

# Effective Treatment of a Melanoma Patient with Hemophagocytic Lymphohistiocytosis after Nivolumab and Ipilimumab Combined Immunotherapy

**Renata Pacholczak-Madej<sup>1,2</sup>, Aleksandra Grela-Wojewoda<sup>1</sup>, Joanna Lompart<sup>1</sup>, Beata Żuchowska-Vogelgesang<sup>1</sup>, Marek Ziobro<sup>1</sup>**

<sup>1</sup>Department of Clinical Oncology, The Maria Skłodowska-Curie National Research Institute of Oncology, Cracow, Poland;

<sup>2</sup>Department of Anatomy, Jagiellonian University Medical College, Cracow, Poland

Received August 23, 2021; Accepted January 31, 2022.

**Key words:** Melanoma – Immune-related adverse events – Hemophagocytic lymphohistiocytosis – Nivolumab and ipilimumab

**Abstract:** Immune checkpoint inhibitors have significantly improved the prognosis of melanoma patients. However, these therapies may trigger unexpected immune-related adverse events (irAEs), which are challenging in making the proper diagnosis and providing treatment. Hematological toxicities are possible irAEs, but were poorly evaluated in clinical trials and treatment recommendations of this specific complications are limited. We present a stage IV melanoma patient who developed an extremely rare toxicity – hemophagocytic lymphohistiocytosis (HLH) after the 4<sup>th</sup> course of combined immunotherapy with nivolumab and ipilimumab. The patient was steroid resistant and only the treatment with various immunosuppressive agents provided control of the disease and finally melanoma regression. In this report, we evaluated the methods of HLH treatment and described our modification of available protocols. Immediate immunosuppression can be life-saving and due to rarity of this condition as well as lack of specific recommendations, every report is valuable for clinicians, especially when treatment was effective.

**Mailing Address:** Marek Ziobro, MD., PhD., Garncarska 11 Street, 31-115 Cracow, Poland; e-mail: mz5@wp.pl

<https://doi.org/10.14712/23362936.2022.4>

© 2022 The Authors. This is an open-access article distributed under the terms of the Creative Commons Attribution License (<http://creativecommons.org/licenses/by/4.0>).

## Introduction

Immune checkpoint inhibitors (ICIs) have changed the treatment landscape of melanoma patients. However, these therapies may trigger unexpected immune-related adverse events (irAEs) with various clinical presentations. The frequency of grade 3/4 (G3/G4) irAEs according to Common Terminology Criteria for Adverse Events (CTCAE) in KEYNOTE-006 occurred in 17% of the patients treated with pembrolizumab, in CheckMate-067 affected 59% and 23% of the patients in nivolumab plus ipilimumab, and nivolumab groups, respectively (Robert et al., 2015; Larkin et al., 2019).

Hematological toxicities are possible irAEs, but were poorly evaluated in clinical trials. In the systematic review the overall incidence of all-grade anemia, neutropenia and thrombocytopenia during anti-programmed cell death (ligand) protein 1 – anti-PD-(L)1 – inhibitors were 9.8%, 0.94%, and 2.8%, respectively. Febrile neutropenia occurred in 0.45% patients (Petrelli et al., 2018). In the analysis of World Health Organization's pharmacovigilance database of individual-case-safety reports (VigiBase), various types of hematologic conditions associated with anti-cytotoxic T lymphocyte antigen-4 (CTLA-4; ipilimumab, tremelimumab), anti-PD-1 (nivolumab, pembrolizumab), and anti-PD-L1 (avelumab, durvalumab, and atezolizumab) treatment were reported, such as: hemolytic anemia (n=68), immune thrombocytopenic purpura (n=57), hemophagocytic lymphohistiocytosis (HLH, n=26), aplastic anemia (n=10), and pure red cell aplasia (n=7) (Davis et al., 2019). HLH was most commonly associated with melanoma (n=15, 58%) during treatment with anti-CTLA-4 therapy (n=13, 50%), occurred earlier (median 26 days), and had a significantly higher rate of fatalities (n=6, 23%) than other hematologic toxicities. Unfortunately, there is no standard treatment for hematologic irAEs which might be potentially fatal, and there were only 2 cases related to anti-CTLA-4 plus anti-PD-1 therapy reported in VigiBase (Davis et al., 2019).

In this case report, we present a patient with advanced melanoma, whose diagnosis of specific irAEs was challenging for our team. The patient developed HLH after the 4<sup>th</sup> course of combined immunotherapy with nivolumab and ipilimumab and was primary resistant to steroids. She required treatment with various immunosuppressive drugs, but luckily, the treatment provided symptom resolution and remission of melanoma. We believe that due to rarity of this condition and lack of specific recommendations, every report is valuable for clinicians, especially when treatment was effective.

## Case report

We report a case of 57-year-old woman with a stage IV B-Raf proto-oncogene (BRAF)-wild-type melanoma with an inoperable tumour in the left groin area (Figure 1A). Due to a good performance status (PS 1) and lack of severe comorbidities, she started the combined immunotherapy with nivolumab (1 mg/kg) and ipilimumab (3 mg/kg). However, after the fourth cycle, the patient's general

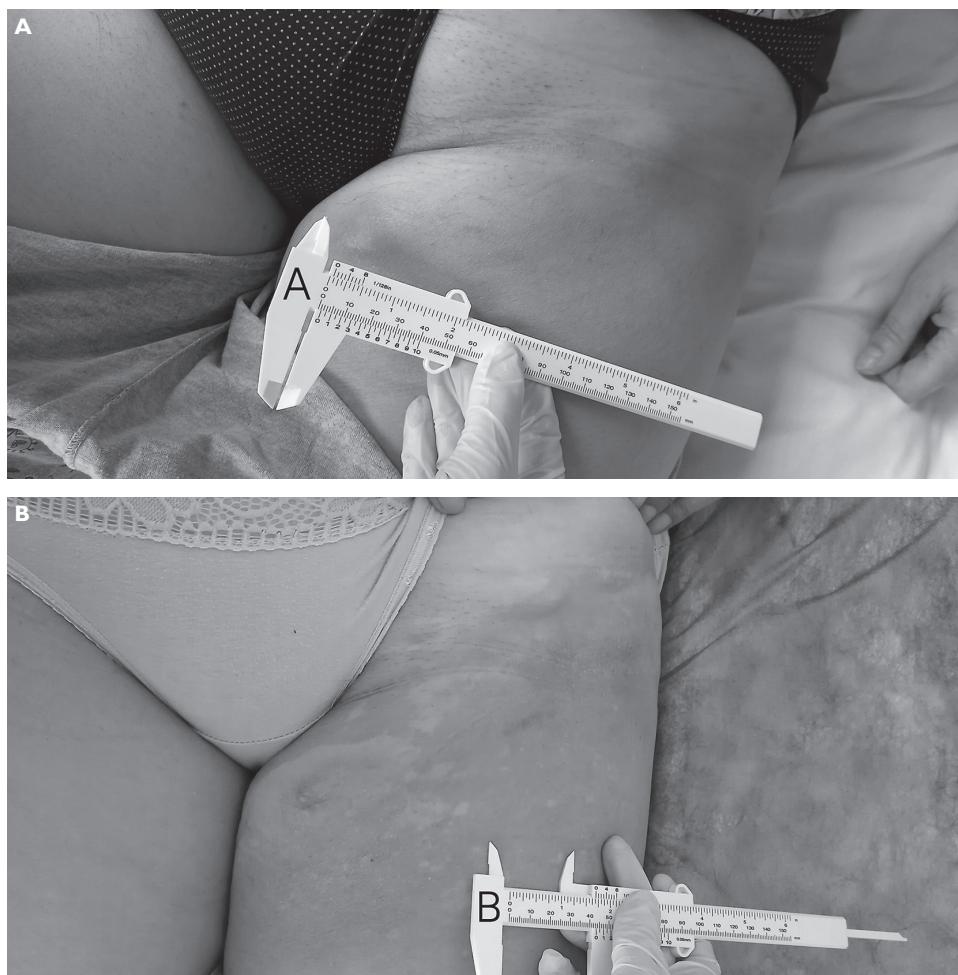


Figure 1 – A) Tumour in the left groin area before the beginning of the treatment, and B) after 4 courses of combined immunotherapy with signs of vitiligo (scale in centimeters).

condition started to deteriorate with persistent, high-spiking fever  $> 40.0\text{ }^{\circ}\text{C}$ , general malaise, dyspnea at rest and elevated markers of inflammation and lactate dehydrogenase (LDH). Having a suspicion of irAEs, we started the initial treatment with prednisone  $1\text{ mg/kg}$  without any improvement. Hence, the patient was admitted to our department for further work-up. Because of the ongoing SARS-CoV-2 pandemic, we excluded coronavirus infection by *polymerase chain reaction* (PCR) test. Remarkable laboratory findings included elevated markers of inflammation (C-reactive protein  $168\text{ ng/ml}$ , procalcitonin  $0.36\text{ ng/ml}$ ) with negative blood cultures, transaminase G3 according to CTCAE, active urinary

**Table 1 – Changes of the basic laboratory parameters during treatment with various immunosuppressive agents**

	Prednisone 1 mg/kg p.o. (day 0–1)	Prednisone 1 g/day iv (day 2–5 with tapering)	MFM 500 mg 3×/day p.o. (day 7–25), 2×/day (day 26–37)	CTX 100–200 mg 1×/day iv (day 10–19)	VP-16 200 mg 2×/week iv (day 18, 22, 26, 30, 37)	Cyclosporine 100 mg 2×/day p.o. (day 26–76)	Day
Hemoglobin, g/dl (12–16)	8.7	8.1	8.4	8.3	7.5	8.4	10.7
Platelet count×10 <sup>9</sup> /l (150–400)	79	112	107	87	88	316	335
CRP, mg/l (<0.5)	168	–	–	–	6.8	12.3	10.1
LDH, U/l (100–214)	1974.2	2448.9	1574.5	1661.9	1492	307.6	206.3
Ferritin, ng/ml (11–282)	–	–	–	7256	–	2242	–
D-dimer, mg/l (<0.5)	48	43.6	8.9	–	–	3.7	–
aPTT, seconds (20–36)	14.7	18.6	25.7	28.8	27.2	20.5	22.7
INR (0.85–1.15)	1.31	1.29	1.12	1.42	1.3	0.94	0.9
Fibrinogen, g/l (1.8–3.5)	1.33	1.17	0.5	<0.6	<0.6	2	5.7

aPTT – activated partial thromboplastin time; CTX – cyclophosphamide; CRP – C-reactive protein; INR – international normalized ratio; iv – intravenous; LDH – lactate dehydrogenase; MFM – mycophenolate mofetil; p.o. – per os, orally; VP-16 – etoposide

sediment, elevated lactate dehydrogenase 2,448.0 U/l, with features of disseminated intravascular coagulation (DIC) – D-dimers 43.6 ng/l, thrombocytes  $79\text{--}112 \times 10^9/l$ , hemoglobin 8.1 g/dl, fibrinogen 1.17 g/l, activated partial thromboplastin time (aPTT) 18.6 seconds, international normalized ratio (INR) 1.29 (reference values are presented in Table 1). In response, we started pulses of methylprednisolone 1,000 mg during 5 days observing amelioration of the patient's condition and symptom remission, but without any major improvement in laboratory parameters with ongoing activation of coagulation (for detailed parameters see Table 1). The patient required a transfusion of fresh frozen plasma in order to prevent her from purpura. Computed tomography (CT) revealed the pleural effusion on the left side and splenomegaly without any evident signs of progression of the disease. We gradually tapered the dose of steroids and introduced mycophenolate mofetil 500 mg 3 times per day and additionally cyclophosphamide 100–200 mg for 9 days with stabilization of platelets, but still an extremely low fibrinogen level. After 15 days of immunosuppressive treatment, we determined the ferritin level which was significantly increased (7,256 ng/ml) together with hypertriglyceridemia of 2.85 mmol/l (reference value < 1.7 mmol/l), splenomegaly in CT scan (12 centimeters). Hence, the patient met 5 out of 8 diagnostic criteria of HLH according to HLH-2004 protocol (Henter et al., 2007) (+ fever, cytopenias in two lines: hemoglobin and platelets) with 98.7% probability of having HLH as estimated using the HLH-probability calculator (HScore, available at: <http://saintantoine.aphp.fr/score/>) (Fardet et al., 2014). We did not perform a bone marrow biopsy due to the high probability of HLH based on abovementioned clinical and laboratory features and unstable coagulation tests. Once the diagnosis was established we started treatment according to the pediatric protocol adding etoposide 200 mg two times per week with our modification (Table 1). After several days of the intensive immunosuppressive treatment, we observed an improvement in laboratory parameters and the patient's full recovery, thereby the patient was discharged after 20 days of hospitalization.

During outpatient treatment, the patient continued the maintenance therapy with reduced dose of mycophenolate mofetil (500 mg two times per day), cyclosporine (100 mg two times per day), low dose of steroids (prednisone 40 mg per day with gradual tapering). We discontinued etoposide after 6 cycles due to neutropenia G2 (CTCAE). As a consequence of life-threatening toxicity G4 (CTACE), the immunotherapy was definitely stopped and the patient remained in observation. She was regularly monitored in our outpatient clinic with clinical features of tumour shrinkage in the left groin area with signs of vitiligo on the left thigh (Figure 1B) and systematic improvement in basic laboratory parameters (Table 1). Immunosuppressive agents were gradually discontinued and finally stopped after 10 weeks since the HLH diagnosis. Additionally, the patient was referred to radiotherapy of the remaining tumour in the left inguinal region. She received 50 Gray (Gy) in 20 fractions using volumetric modulated arc therapy (VMAT).

CT scan performed 3 months after discontinuation of immunotherapy revealed a partial remission of the tumour. The patient remains in a good clinical condition and remission of melanoma.

## Discussion

HLH is a disease on the spectrum of cytokine storm syndrome with uncontrolled inflammation, which might be fatal in case of an incorrect treatment. We may distinguish two types: primary HLH – in which a genetic defect causes a lack of cytotoxic activity of T lymphocytes and natural killer cells, and acquired – associated with infections, malignancies, and autoinflammatory disorders (Machowicz and Basak, 2020). Nowadays, an additional triggering factor is the treatment with ICLs, when we purposely release the blockade of the immune system.

The name HLH comes from hemophagocytosis, which is the phagocytosis of blood cells by activated macrophages observed in the bone marrow smear or in cytology from the other, involved organ. However, confirmation of its presence is neither required nor sufficient for the diagnosis of HLH, because not all patients have hemophagocytosis at disease onset (Gupta et al., 2008). Due to the rapid onset and often fulminant progress, diagnosis should not be delayed by looking for this single feature. Jordan et al. (2011) considered hemophagocytosis as the less important diagnostic criteria. Hence, we did not perform the bone marrow biopsy in the presented case. The diagnosis of HLH is made on the basis of clinical and laboratory features (HLH-2004 diagnostic criteria), such as: fever, splenomegaly, cytopenia in  $\geq 2$  lines (neutrophils  $< 1.0 \times 10^9/l$ ; hemoglobin  $< 9$  g/dl; platelet count  $< 100 \times 10^9/l$ ), hypofibrinogenemia ( $\leq 1.5$  g/l [150 mg/dl]) and/or hypertriglyceridemia ( $\geq 3$  mmol/l [265 mg/dl]), hemophagocytosis, ferritin  $\geq 500$  ng/ml, low NK-cell activity, soluble cluster of differentiation 25 (sCD25/soluble interleukin 2 receptor)  $\geq 2,400$  U/ml with fulfilment of at least 5 out of 8 (La Rosée et al., 2019). Soluble CD25 is a useful marker of inflammation, but is not available at our institution, similarly to NK-cell activity. However, even without these parameters, fulfilment of the remaining criteria was sufficient to establish the proper diagnosis.

The treatment of HLH depends on the underlying trigger and severity of symptoms. General recommendation states that in case of rapid deterioration of the patient's methylprednisolone pulses or dexamethasone  $10$  mg/m<sup>2</sup> should be initiated with or without intravenous immunoglobulins (1.6 g/kg split over 2–3 days) (Machowicz and Basak, 2020). This approach may be sufficient in moderate HLH. In more severe cases the standards of treatment are protocols adopted from the pediatric population – HLH-94 and HLH-2004 (Henter et al., 2007; La Rosée et al., 2019). Both of these regimens are based on etoposide ( $2 \times 150$  mg/m<sup>2</sup>/week 1–2, and  $1 \times 150$  mg/m<sup>2</sup>/week 3–8), dexamethasone ( $10$  mg/m<sup>2</sup> with tapering dose) and cyclosporine (aiming at blood levels of around 200 µg/l). The main difference is the initiation of cyclosporine – concomitantly from the beginning of the treatment (in HLH-2004) or as a maintenance after 8 weeks (in HLH-94) (Henter et al., 2007;

La Rosée et al., 2019). Due to the toxicity of HLH-94 protocol in adults, Henter et al. (2006) proposed a reduction of the etoposide dose to 50–100 mg/m<sup>2</sup> administered once per week.

Unfortunately, there is a lack of specific recommendations for ICI-related HLH. European Society of Medical Oncology recommends the initiation of high-dose corticosteroids and other immunosuppressive drugs with close collaboration with a hematologist (Haanen et al., 2017). In the literature there are available case reports in which treatment interruption or corticosteroids alone were used with sufficient response (Sadaat and Jang, 2018; Mizuta et al., 2020; Gambichler et al., 2021). In melanoma patients HLH can be also attributed to a solid tumour as a first presentation of the disease (Stabler et al., 2017), Epstein-Barr virus (EBV) infection (Davis et al., 2019) and can be associated with BRAF/MEK inhibitors (Samaran et al., 2020; Dudda et al., 2021). These cases represented rather moderate HLH where treatment discontinuation, basic supportive care (intravenous rehydration and paracetamol), and low dose steroids (or even without steroids prescription) (Samaran et al., 2020) were sufficient methods of treatment. In 19% of cases in VigiBase, concomitant Epstein-Barr virus infection was reported, suggesting a potentially augmented immune response in case of chronic underlying infection (Davis et al., 2019). Paradoxically, nivolumab has been also used in the treatment of relapsed/refractory EBV-associated HLH (Liu et al., 2020). In the presented case, the patient was steroid-refractory and only the treatment with HLH-2004 protocol with our modification – an additional short course of cyclophosphamide with cyclosporine and mycophenolate as maintenance, provided control of the disease.

## Conclusion

Immune-related adverse events can be challenging in making diagnosis. Although HLH is potentially fatal disease, it can be recognized by some easily accessible laboratory parameters. Diagnostic procedures should not delay immediate administration of high dose steroids, which in many cases is a sufficient treatment. However, some patients can be steroid-refractory and require additional treatment with immunosuppressive agents. Proper immunosuppression can be life-saving and in spite of the immunotherapy withdrawal may provide melanoma regression as in the presented patient.

## References

- Davis, E. J., Salem, J., Young, A., Green, J. R., Ferrell, P. B., Ancell, K. K., Johnson, D. B. (2019) Hematologic complications of immune checkpoint inhibitors. *Oncologist* **24(5)**, 584–588.
- Dudda, M., Mann, C., Heinz, J., Schmidgen, I., Weid, F., Kühn, M., Loquai, C. (2021) Hemophagocytic lymphohistiocytosis of a melanoma patient under BRAF/MEK-inhibitor therapy following anti-PD1 inhibitor treatment: A case report and review to the literature. *Melanoma Res.* **31(1)**, 81–84.
- Fardet, L., Galicier, L., Lambotte, O., Marzac, C., Aumont, C., Chahwan, D., Hejblum, G. (2014) Development and validation of the HScore, a score for the diagnosis of reactive hemophagocytic syndrome. *Arthritis Rheumatol.* **66(9)**, 2613–2620.

- Gambichler, T., Rached, N. A., Nowack, N., Behle, B., Susok, L. (2021) Hemophagocytic lymphohistiocytosis after initiation of combined immunotherapy for metastatic melanoma. *Ann. Hematol. Oncol.* **8(4)**, 1337.
- Gupta, A., Weitzman, S., Abdelhaleem, M. (2008) The role of hemophagocytosis in bone marrow aspirates in the diagnosis of hemophagocytic lymphohistiocytosis. *Pediatr. Blood Cancer* **50(2)**, 192–194.
- Haanen, J. B. A. G., Carbone, F., Robert, C., Kerr, K. M., Peters, S., Larkin, J., Jordan, K. (2017) Management of toxicities from immunotherapy: ESMO Clinical Practice Guidelines for diagnosis, treatment and follow-up. *Ann. Oncol.* **28**, iv119–iv142 (Suppl. 4).
- Henter, J. I., Horne, A., Aricó, M., Egeler, R. M., Filipovich, A. H., Imashuku, S., Ladisch, S., McClain, K., Webb, D., Winiarski, J., Janka, G. (2007) HLH-2004: Diagnostic and therapeutic guidelines for hemophagocytic lymphohistiocytosis. *Pediatr. Blood Cancer* **48(2)**, 124–131.
- Henter, J. I., Chow, C. B., Leung, C. W., Lau, Y. L. (2006) Cytotoxic therapy for severe avian influenza A (H5N1) infection. *Lancet* **367(9513)**, 870–873.
- Jordan, M. B., Allen, C. E., Weitzman, S., Filipovich, A. H., McClain, K. L. (2011) How I treat hemophagocytic lymphohistiocytosis. *Blood* **118(15)**, 4041–4052.
- La Rosée, P., Horne, A., Hines, M., von Bahr Greenwood, T., Machowicz, R., Berliner, N., Birndt, S., Gil-Herrera, J., Girschikofsky, M., Jordan, M. B., Kumar, A., van Laar, J. A. M., Lachmann, G., Nichols, K. E., Ramanan, A. V., Wang, Y., Wang, Z., Janka, G., Henter, J. I. (2019) Recommendations for the management of hemophagocytic lymphohistiocytosis in adults. *Blood* **133(23)**, 2465–2477.
- Larkin, J., Chiarion-Sileni, V., Gonzalez, R., Grob, J.-J., Rutkowski, P., Lao, C. D., Wolchok, J. D. (2019) Five-year survival with combined nivolumab and ipilimumab in advanced melanoma. *N. Engl. J. Med.* **381(16)**, 1535–1546.
- Liu, P., Pan, X., Chen, C., Niu, T., Shuai, X., Wang, J., Liu, T. (2020) Nivolumab treatment of relapsed/refractory Epstein-Barr virus-associated hemophagocytic lymphohistiocytosis in adults. *Blood* **135(11)**, 826–833.
- Machowicz, R., Basak, G. (2020) How can an internal medicine specialist save a patient with hemophagocytic lymphohistiocytosis (HLH)? *Pol. Arch. Intern. Med.* **130(5)**, 431–437.
- Mizuta, H., Nakano, E., Takahashi, A., Koyama, T., Namikawa, K., Yamazaki, N. (2020) Hemophagocytic lymphohistiocytosis with advanced malignant melanoma accompanied by ipilimumab and nivolumab: A case report and literature review. *Dermatol. Ther.* **33(3)**, e13321.
- Petrelli, F., Ardito, R., Borgonovo, K., Lonati, V., Cabiddu, M., Ghilardi, M., Barni, S. (2018) Haematological toxicities with immunotherapy in patients with cancer: A systematic review and meta-analysis. *Eur. J. Cancer* **103**, 7–16.
- Robert, C., Schachter, J., Long, G. V., Arance, A., Grob, J. J., Mortier, L., Ribas, A. (2015) Pembrolizumab versus ipilimumab in advanced melanoma. *N. Engl. J. Med.* **372(26)**, 2521–2532.
- Sadaat, M., Jang, S. (2018) Hemophagocytic lymphohistiocytosis with immunotherapy: Brief review and case report. *J. Immunother. Cancer* **6(1)**, 49.
- Samaran, Q., Belakebi, D., Theret, S., Becquart, O., Girard, C., Du Thanh, A., Guillot, B., Lesage, C., Dereure, O. (2020) Hemophagocytic lymphohistiocytosis in advanced melanoma treated with dabrafenib and trametinib combination: two cases. *Melanoma Res.* **30(5)**, 519–523.
- Stabler, S., Becquart, C., Dumezy, F., Terriou, L., Mortier, L. (2017) Hemophagocytic lymphohistiocytosis in patients with metastatic malignant melanoma. *Melanoma Res.* **27(4)**, 377–379.

# Pneumomediastinum: A Rare Complication of Endobronchial Ultrasound Guided Fine Needle Aspiration

**Biplab K. Saha**

Department of Pulmonary and Critical Care Medicine, Ozarks Medical Center, West Plains, USA

Received November 9, 2020; Accepted January 31, 2022.

**Key words:** EBUS-TBNA – Pneumomediastinum – Complications

**Abstract:** Endobronchial ultrasound guided transbronchial needle aspiration (EBUS-TBNA) is a commonly performed outpatient procedure used for the diagnosis, staging of lung cancer, and the evaluation of thoracic lymphadenopathy of unknown origin. With the advent of this minimally invasive technology, mediastinoscopy, once the gold standard, has fallen out of favour. Pneumomediastinum is a rare complication of EBUS-TBNA and can often be managed conservatively. We present a case of a 52-year-old female who developed pneumomediastinum following EBUS-TBNA and improved with expectant management in the emergency department. We discuss the proposed pathophysiology of this rare occurrence that usually follows a benign course. Severe complications, such as mediastinitis and tracheal tear, need to be excluded promptly.

**Mailing Address:** Biplab K. Saha, MD., Ozarks Medical Center, 1100 Kentucky Avenue, West Plains, Missouri 65775, USA; e-mail: spanophilic@yahoo.com

<https://doi.org/10.14712/23362936.2022.5>

© 2022 The Author. This is an open-access article distributed under the terms of the Creative Commons Attribution License (<http://creativecommons.org/licenses/by/4.0>).

## Introduction

Pneumomediastinum is a commonly encountered medical condition in the emergency department (ED). It can occur in isolation or be associated with pneumothorax. Common causes of pneumomediastinum are blunt force trauma to the chest, obstructive pulmonary diseases, and mediastinitis, which occurs most frequently as an iatrogenic complication of upper aero-digestive tract procedures. Endobronchial ultrasound guided transbronchial needle aspiration (EBUS-TBNA) refers to the performance of fine needle aspiration of the target lesion under direct ultrasound visualization during bronchoscopy. EBUS-TBNA is currently the procedure of choice for diagnosis and staging of lung cancer due to the minimal invasiveness (Vyas et al., 2013). EBUS-TBNA allows sampling of most hilar and mediastinal lymph nodes except paraaortic and paraesophageal lymph node stations (stations 5, 6, 8, and 9). However, simultaneous endoscopic ultrasound using EBUS scope (EUS-B) enables the operator to access the lower mediastinal lymph node stations (stations 8 and 9) by a transesophageal approach. EUS-B guided fine needle aspiration (EUS-NA) provides a more complete staging of the mediastinum with increased sensitivity and negative predictive value (Bugalho et al., 2018). The procedure is usually performed as an outpatient with minimal risk of complications. Pneumomediastinum is a rare complication of EBUS-TBNA that has been reported in the form of case reports in the literature. The pathophysiology behind the causation of pneumomediastinum is unclear, and most patients follow a benign trajectory. We report the rare occurrence of pneumomediastinum in a patient following EBUS-TBNA, who improved with conservative management. The proposed pathophysiology and management are also discussed.

## Case report

A 52-year-old female presented to the hospital with intermittent anterior chest pain and self-reported episodes of hemoptysis of several months duration. The patient was an active smoker with more than thirty-five pack-year history of smoking. She was treated with antibiotics multiple times in the recent past for recurrent pneumonia. On admission, her vital signs were stable. Physical examination was unremarkable. She underwent a computed tomographic angiogram of the chest to rule out pulmonary embolism. Computed tomography (CT) of the chest revealed hilar and mediastinal lymphadenopathy, and concerns were raised regarding the possibility of lymphoma or a primary lung malignancy. The patient underwent EBUS-TBNA of right lower paratracheal (4R), subcarinal (7) and right hilar (10R) lymph node stations. The procedure was performed under general anesthesia using a 21g needle. Low tidal volume ventilation with positive end-expiratory positive pressure (PEEP) of 5 cm of water was used throughout the procedure. Care was taken to avoid the development of auto-PEEP. There was no endobronchial lesion, and the TBNA was uneventful. There was minimal bleeding. The patient was discharged home in a stable condition following the procedure. However, the patient



Figure 1 – Coronal computed tomography scan of the chest revealing pneumomediastinum with extension at the base of the neck.

presented to the ED that night with worsening chest pain and difficulty breathing. Her vital signs on presentation were a blood pressure of 147/88 mm Hg, a pulse rate of 93 beats per minute, a temperature of 36.83 °C, a respiratory rate of 17 breaths per minute, and oxygen saturation of 96% with the patient breathing ambient air. Physical examination revealed a non-toxic patient in no acute distress. The remainder of the physical examination, including chest auscultation, was completely normal. A chest X-ray was unremarkable. Representative slides of the CT scan of the chest are shown in Figures 1 and 2. The coronal (Figure 1) and axial (Figure 2) views revealed pneumomediastinum with an extension of the air up to the base of the neck. There was no evidence of mediastinitis on transverse imaging. A gastrografin esophagram revealed no esophageal perforation. The patient was

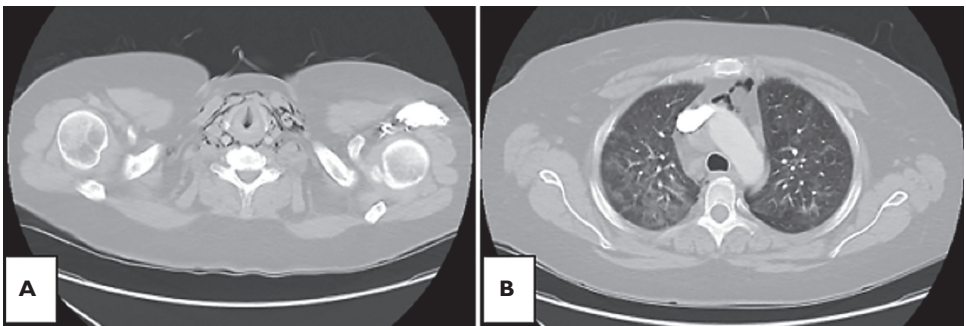


Figure 2 – Axial computed tomography scan on the chest at the level of the vocal cords (A) and upper trachea (B) showing varying degrees of air around the airways and vascular structures.

treated with pain medication with subsequent improvement of her symptoms. She was discharged home from the ED with a planned follow-up with the pulmonologist. The lymph node fine needle aspirations (FNAs) were negative for malignancy.

## Discussion

This case represents a rare complication of EBUS-TBNA. EBUS-TBNA has revolutionized lung cancer diagnosis and simultaneous staging. It is a sensitive, safe, and less invasive procedure compared to mediastinoscopy and has largely replaced the later in the diagnostic algorithm of lung cancer. Complications from EBUS-TBNA are rare and mostly involve mild bleeding (Asano et al., 2013). Only a handful of cases of isolated pneumomediastinum have been reported in the literature, in the form of case reports (Piroddi et al., 2017). A review of all published trials of EBUS-TBNA between 1995–2012 did not show any case of pneumomediastinum (von Bartheld et al., 2014). Similarly, in a nationwide study from Japan, there was no report of pneumomediastinum (Asano et al., 2013). The exact pathophysiologic mechanism of pneumomediastinum following TBNA is unclear. One possible explanation is the Macklin effect. Macklin effect refers to the development of pneumomediastinum due to increased intrathoracic pressure. The increased intrathoracic pressure leads to alveolar rupture and forceful expulsion of the alveolar air in the mediastinal space following centripetal dissection along the bronchovascular bundle (Macklin and Macklin, 1944). Pneumomediastinum can be seen in patients with blunt force trauma to the chest, following forceful coughing or sneezing, and in the setting obstructive pulmonary diseases. This can occur with or without accompanying pneumothorax.

EBUS-TBNA utilizes the application of small caliber needles for the purpose of lymph node sampling under direct ultrasound visualization. The procedure is generally safe and well-tolerated by patients. The risk of pneumothorax following EBUS-TBNA has been reported to be 0.03% (Asano et al., 2013). Significant trauma to the airways leading to leakage of air is therefore highly unlikely. The etiology of the pneumomediastinum in our case is unclear. The patient underwent the procedure under general anesthesia with low tidal volume ventilation and low PEEP, thus, making barotrauma an unlikely causative etiology. Similarly, there was no coughing, breath stacking, or auto-PEEP generation, which could have increased the intrathoracic pressure. As a result, it is plausible that in very rare occasions, FNA during EBUS can in fact cause isolated pneumomediastinum by the creation of temporary and self-limited tracheomediastinal or bronchomediastinal fistula.

Pneumomediastinum following TBNA should be managed conservatively. However, it is important to rule out mediastinitis, as this can be rapidly fatal in the absence of prompt intervention (Pastene et al., 2020). Whether pneumomediastinum represents a rare or a relatively underdiagnosed complication – due to lack of significant symptoms – is unknown. Patients might not seek medical attention due to mild chest discomfort following bronchoscopy, which could be

the sole manifestation of pneumomediastinum. In addition, chest X-ray might be relatively insensitive to identify mild cases, as was the case in our patient (Zylak et al., 2000). Knowledge of this unusual complication is crucial for clinicians to prevent unnecessary surgical interventions, such as chest tube insertion. At the same time, careful evaluation is necessary to exclude serious damage to the upper airway structure, such as esophageal perforation and tracheal tear. Bronchomediastinal fistula and mediastinitis following EBUS-TBNA have been reported (Bougioukas et al., 2019).

## References

- Asano, F., Aoe, M., Ohsaki, Y., Okada, Y., Sasada, S., Sato, S., Suzuki, E., Semba, H., Fukuoka, K., Fujino, S., Ohmori, K. (2013) Complications associated with endobronchial ultrasound-guided transbronchial needle aspiration: A nationwide survey by the Japan Society for Respiratory Endoscopy. *Respir. Res.* **14(1)**, 50.
- Bougioukas, I., Seipelt, R., Huwer, H. (2019) Bronchial fistula and pneumomediastinum after EBUS-TBNA following mediastinoscopy. *Thorac. Cardiovasc. Surg. Rep.* **8(1)**, e11–e13.
- Bugalho, A., de Santis, M., Szlubowski, A., Rozman, A., Eberhardt, R. (2018) Trans-esophageal endobronchial ultrasound-guided needle aspiration (EUS-B-NA): A road map for the chest physician. *Pulmonology* **24(1)**, 32–41.
- Macklin, M. T., Macklin, C. C. (1944) Malignant interstitial emphysema of the lungs and mediastinum as an important occult complication in many respiratory diseases and other conditions: An interpretation of the clinical literature in the light of laboratory experiment. *Medicine* **23(4)**, 281–358.
- Pastene, B., Cassir, N., Tankel, J., Einav, S., Fournier, P.-E., Thomas, P., Leone, M. (2020) Mediastinitis in the intensive care unit patient: A narrative review. *Clin. Microbiol. Infect.* **26(1)**, 26–34.
- Piroddi, I. M. G., Gatto, P., Perazzo, A., Barlascini, C., Nicolini, A. (2017) Pneumomediastinum following endobronchial ultrasound-guided transbronchial needle aspiration: A case report. *Tanaffos* **16(3)**, 245–247.
- von Bartheld, M. B., van Breda, A., Annema, J. T. (2014) Complication rate of endosonography (endobronchial and endoscopic ultrasound): A systematic review. *Respiration* **87(4)**, 343–351.
- Vyas, K. S., Davenport, D. L., Ferraris, V. A., Saha, S. P. (2013) Mediastinoscopy: Trends and practice patterns in the United States. *South. Med. J.* **106(10)**, 539–544.
- Zylak, C. M., Standen, J. R., Barnes, G. R., Zylak, C. J. (2000) Pneumomediastinum revisited. *Radiographics* **20(4)**, 1043–1057.

# Parvovirus B19 Intrauterine Infection and Eventration of the Diaphragm

**Georgios Mitsiakos<sup>1</sup>, Christoforos Gavras<sup>1</sup>, Georgios N. Katsaras<sup>1</sup>, Ilias Chatziioannidis<sup>1</sup>, Vasilios Mouravas<sup>2</sup>, Christina Mitsiakou<sup>1</sup>, Vasilios Lampropoulos<sup>2</sup>, Nikolaos Nikolaidis<sup>1</sup>**

<sup>1</sup><sup>2</sup><sup>nd</sup> Neonatal Department and Neonatal Intensive Care Unit, Aristotle University of Thessaloniki, “Papageorgiou” General Hospital of Thessaloniki, Thessaloniki, Greece; <sup>2</sup><sup>2</sup><sup>nd</sup> Department of Pediatric Surgery, Aristotle University of Thessaloniki, “Papageorgiou” Hospital, Thessaloniki, Greece

Received November 22, 2021; Accepted January 31, 2022.

**Key words:** Diaphragmatic eventration – Neonate – Fetus – Parvovirus B19

**Abstract:** Parvovirus B19 infection in pregnancy may have a poor outcome for the fetus. Ocular anomalies, brain damage with hydrocephalus and central nervous system (CNS) scarring, cleft lip and hypospadias, as well myocarditis and congenital heart disease have been reported. We present a case of a preterm female neonate born with ascites, hydrothorax and congenital diaphragmatic eventration (CDE), with a prenatal diagnosis of congenital diaphragmatic hernia (CDH). The neonate was born prematurely at 32 weeks gestation with caesarean section due to a previous caesarean delivery. She was immediately intubated in the delivery room, transferred in the Neonatal Intensive Care Unit (NICU) and supported with high frequency oscillatory ventilation (HFOV). The diagnosis of CDH was sonographically estimated from the 20<sup>th</sup> week of gestation and surgical correction was decided. During surgery CDE was diagnosed instead of CDH and despite postoperatively care the neonate developed disseminated intravascular coagulation and finally died in the 40<sup>th</sup> hour of life. Along with the identification of parvovirus B19 in the pleural fluid by PCR, the biopsy of the diaphragm revealed connective tissue, full of vasculature and absence muscle tissue. Although only cytomegalovirus, rubella, and toxoplasmosis were considered to be associated with CDE, parvovirus B19 might also be related to this congenital diaphragmatic malformation. In CDE, the function of the lungs can be compromised as a consequence of the compression applied by the abdominal organs. The neonatologists should include this condition in their differential diagnosis for a more direct and effective management.

**Mailing Address:** Assoc. Prof. Georgios Mitsiakos, MD., PhD., Ring Road, Nea Efkarpia 56403, Thessaloniki, Greece; Phone: 0030 231 332 336; Mobile Phone: 0030 697 472 89 79; e-mail: mitsiakos@auth.gr

<https://doi.org/10.14712/23362936.2022.6>

© 2022 The Authors. This is an open-access article distributed under the terms of the Creative Commons Attribution License (<http://creativecommons.org/licenses/by/4.0>).

## Introduction

Human parvovirus B19 was first identified by Cossart et al. in 1975 in the serum of normal blood bank donors after being screened for the hepatitis B virus. In 1983, Anderson et al. reported parvovirus B19 as the probable cause of erythema infectiosum, also known as fifth disease. The first association of parvovirus B19 infection in pregnancy with poor outcome was in 1984, when hydropic fetuses were shown to have anti-B19 immunoglobulin M (IgM) (Brown et al., 1984). Multiple studies regarding congenital infections have confirmed this association (Matsunaga et al., 1987; Maeda et al., 1988; Sahakian et al., 1991; Faure et al., 1996; Mielke and Enders, 1996). Congenital diaphragmatic eventration (CDE) is generally defined as an abnormal displacement of a portion or whole of an attenuated but otherwise intact diaphragm into the thoracic cavity. Clinically it mimics the features of congenital diaphragmatic hernia (CDH) with displacement of abdominal organs into the thorax (Clifton and Wulkan, 2017).

We hereby present a case of a preterm female neonate born with ascites, hydrothorax and congenital diaphragmatic eventration (CDE).

## Case report

A female neonate was prematurely born after 32 weeks of gestation with caesarean section due to a previous caesarean delivery. She was immediately intubated in the delivery room and afterwards she then transferred in the Neonatal Intensive Care Unit (NICU), where support with high frequency oscillatory ventilation (HFOV) was provided. Surfactant was administered and iNO treatment was initiated. The hematologic and biochemical investigations upon admission were normal, except for a moderate anaemia (Table 1).

A chest X-ray verified the existence of right congenital diaphragmatic hernia in accordance with the pre-existing ultrasound diagnosis of CDH at the 20<sup>th</sup> week of gestation. The chest X-ray revealed a bowel gas pattern and herniation of the liver

**Table 1 – Hematologic and biochemical investigations**

WBC	8,130/ $\mu$ l	Urea	17 mg/dl
Gr	32.7%	Creatinine	0.70 mg/dl
Ly	50.9%	K	3.85 mmol/l
Mo	8.4%	Na	133.3 mmol/l
Eo	1.1%	Cholesterol	100 mg/dl
RBC	3.14 $\times$ 10 <sup>6</sup> / $\mu$ l	Triglyceride	19 mg/dl
Hb	12.1 g/dl	Total bilirubin	1.78 mg/dl
Hct	37.3%	SGOT	69 IU/l
PLT	295,000/ $\mu$ l	SGPT	6 IU/l

Eo – eosinophils; Gr – granulocytes; Hb – haemoglobin; Hct – haematocrit; Ly – lymphocytes; Mo – monocytes; PLT – platelet count; RBC – red blood cell count; WBC – white blood cell count; SGOT – serum glutamic-oxaloacetic transaminase; SGPT – serum glutamic-pyruvic transaminase

**Table 2 – Biochemical examination of the pleural fluid**

Volume	55 ml	
Hue	yellow, slightly opaque	
Cells	5,070/ $\mu$ l	
Lymphocytes	majority protein	2.02 g/dl
Albumin	1.59 g/dl	
LDH	82 U/l	
Glucose	63 mg/dl	
Amylase	6 U/l	

LDH – lactate dehydrogenase

in the right hemithorax (Figure 1). Upper gastrointestinal (GI) series showed the small intestine in the thoracic cavity (Figure 2A and B). Echocardiography revealed a patent ductus arteriosus and an atrial septal defect with right-left leakage. 55 ml of pleural fluid were drained from the right side. Pleural fluid biochemical analysis was compatible with a transudate (Table 2), while PCR testing identified parvovirus B19 genome. Both pleural fluid and blood cultures were negative. Diaphragm biopsy was consistent with a connective tissue, full of vasculature and lacking muscle tissue (Figure 3A and B).

It was then decided to proceed to surgery via an abdominal incision. On the table, a CDE diagnosis was established instead of the assumed diagnosis of CDH. Therefore, the initial plan changed, and the diaphragm was plicated with four rows of 3-0 Prolene sutures.

Dramatic deterioration of the clinical condition due to a disseminated intravascular coagulation (DIC) developed post operatively and the neonate died within few

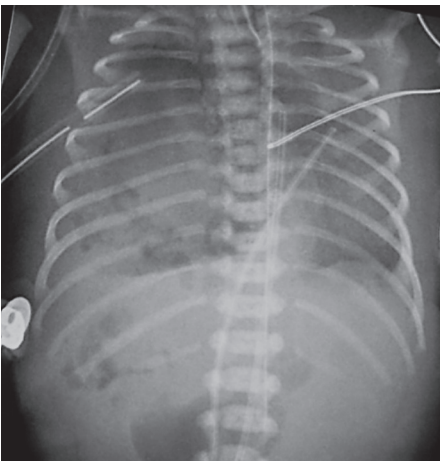


Figure 1 – First chest X-ray: a bowel gas pattern in the right hemithorax and herniation of the liver.

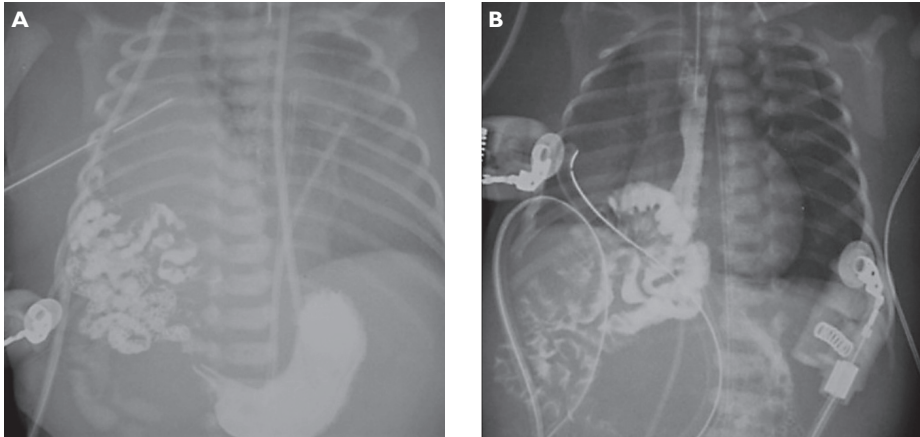


Figure 2 – Gastrointestinal passage examination: small intestine is delineated in the thoracic cavity.

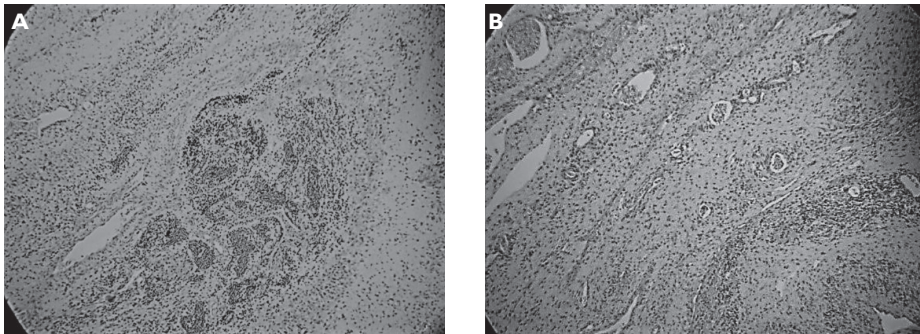


Figure 3 – Histological septal incisions characterized by lack of muscle cells, loose connective tissue, rich vascularity and lymphocytic infiltrations.

hours – just after 40 hours of life. Because of that outcome we couldn't further investigate for potential genetic syndromes with severe malformations.

## Discussion

The diaphragm develops from four embryologic structures: the septum transversum, pleuroperitoneal membranes, the dorsal mesentery of the oesophagus and body wall muscles. The diaphragm develops between the 8<sup>th</sup> and 10<sup>th</sup> week and divides the coelomic cavity into a pleural and a peritoneal space. The aetiology of CDE is postulated to be the abnormal migration of myoblasts into septum transversum and pleuroperitoneal membrane when the midgut returns prematurely from its extracoelomic herniation to the peritoneal cavity before week ten of gestation (Tarver et al., 1984).

The eventration process can have varying degrees of diaphragmatic involvement. Histologically a thin muscle plate or even complete absence of muscles might be found. In the latter cases the thin membrane is characterized by the presence of three layers: one composed of mesothelial cells representing the pleura, a layer of diffuse fibrous tissues representing the malformed diaphragm and a third layer representing the peritoneum (Tarver et al., 1984; Schumpelick et al., 2000; Soni et al., 2005).

Diaphragmatic eventration accounts for about 5% of all diaphragmatic anomalies (Saleh et al., 2012). Complete eventrations tend to be more frequent in males and left sided, whereas partial forms are more often described on the right side (Christensen, 1959). Diaphragmatic eventration can be classified as congenital or acquired. The *acquired type* occurs as a consequence of phrenic nerve injury, while the *congenital* is due to incomplete or absent muscularization of the pleuroperitoneal membrane during intrauterine development (Clifton and Wulkan, 2017; Pradhan et al., 2020).

Parvovirus B19 is a small, single-stranded, non-enveloped DNA virus of the *Parvoviridae* family. Parvovirus B19 has a predilection for rapid division of cells such as red blood cells, affecting the final stage of their maturation, causing both haemolysis and red blood cell aplasia. The P antigen on red blood cells is a cellular receptor of the parvovirus B19. Only 1 in 200,000 humans is P negative and those persons are resistant to parvovirus B19 infection (Heegaard and Brown, 2002).

The teratogenicity of parvovirus has not yet been fully determined, although fetal malformations have been occasionally reported. Ocular anomalies, brain damage with hydrocephalus and central nervous system (CNS) scarring, cleft lip and hypospadias have been reported in association with acute intrauterine parvovirus B19 infection. Myocarditis and congenital heart disease (e.g. ventricular septal defect) have been described as well (Matsunaga et al., 1987; Sahakian et al., 1991; Tiessen et al., 1994; Mielke and Enders, 1996; Konstantinidou et al., 2007; Masini et al., 2017). Like canine parvovirus in puppies, B19 virus seems to have an affinity for fetal muscle cells, as can be concluded from findings in the heart, skeletal muscle, and umbilical artery. The reason why the heart tissue and the arteries are particularly damaged is not clearly understood. A plausible explanation could be that it might be related to a focal endothelial damage, in the way parvovirus infection manifests in swine and rat. Moreover, skeletal muscle tissue seems to be more generally affected (Hartwig et al., 1989). To our knowledge the association of CDE and intrauterine parvovirus B19 infection has not been previously described.

Most women are immune to parvovirus B19 before pregnancy (Barros De Freitas et al., 1999; Di Domenico et al., 2002; Ornoy and Ergaz, 2017). During pregnancy the risk of acquired parvovirus B19 infection is quite low, ranging from 0 to 16.5% (Barros De Freitas et al., 1999; Makhseed et al., 1999; Tolfvenstam et al., 2001; Di Domenico et al., 2002; Baschat et al., 2003). The prevalence of maternal infection is higher during epidemics, with seroconversion rate ranging

from 3 to 34% (Woernle et al., 1987; Kerr et al., 1994). The risk of adverse fetal outcome is increased if maternal infection occurs during the first two trimesters of pregnancy and far more rarely during the third trimester (Ornoy and Ergaz, 2017). The transmission rate of maternal parvovirus B19 infection to the fetus is 17 to 33% (Gratacós et al., 1995). Although parvovirus has no adverse effects on the healthy pregnant mother, its transplacental transmission to the fetus is an important cause of intrauterine death, abortion and stillbirth. These outcomes can occur after symptomatic or asymptomatic maternal infection. The virus infects liver which is the main site of erythrocyte production in the embryo (Ornoy and Ergaz, 2017). The fetus is more vulnerable during the second trimester as the liver is the main source of hematopoietic activity and red blood cells half-life of is short (50–75 days) in comparison to later hematopoietic stages. Severe anaemia can lead to congestive heart failure and development of hydrops fetalis. The risk of fetal complications – as mentioned above – depends largely upon gestational age at the time of maternal infection with parvovirus B19. Maternal infection during the first 9–16 weeks of pregnancy carries the highest risk for fetal loss; it is largely reduced during the second half of pregnancy and even more in the last 2 months (Yaegashi et al., 1994; Nyman et al., 2002). In our case, the neonate had severe hydrops fetalis with mild anaemia, probably because the cause of the ascites wasn't the anaemia but the CDE. Although the nature of this pathology is not well known, the pathogenesis of hydrops in fetuses with malformations like CDH is considered secondary to the obstruction of the superior and inferior venae cavae in addition to the hepatic venous returns (Sydorak et al., 2002; Shojai et al., 2004; Rossi et al., 2014).

## Conclusion

The complex development of the diaphragm plays a direct role on the occurrence of congenital diaphragmatic pathologies. In CDE, lung function can be heavily compromised by the abdominal organ compression applied. Neonatologists should be familiar with this clinical condition and include it in their differential diagnosis for a more direct and effective management.

## References

- Anderson, M. J., Jones, S. E., Fisher-Hoch, S. P., Lewis, E., Hall, S. M., Bartlett, C. L., Cohen, B. J., Mortimer, P. P., Pereira, M. S. (1983) Human parvovirus, the cause of erythema infectiosum (fifth disease)? *Lancet* **1(8338)**, 1378.
- Barros De Freitas, R., Buarque De Gusmão, S. R., Durigon, E. L., Linhares, A. C. (1999) Survey of parvovirus B19 infection in a cohort of pregnant women in Belém, Brazil. *Braz. J. Infect. Dis.* **3(1)**, 6–14.
- Baschat, A. A., Towbin, J., Bowles, N. E., Harman, C. R., Weiner, C. P. (2003) Prevalence of viral DNA in amniotic fluid of low-risk pregnancies in the second trimester. *J. Matern. Fetal Neonatal Med.* **13(6)**, 381–384.
- Brown, T., Anand, A., Ritchie, L. D., Clewley, J. P., Reid, T. M. (1984) Intrauterine parvovirus infection associated with hydrops fetalis. *Lancet* **2(8410)**, 1033–1034.
- Christensen, P. (1959) Eventration of the diaphragm. *Thorax* **14(4)**, 311–319.

- Clifton, M. S., Wulkan, M. L. (2017) Congenital diaphragmatic hernia and diaphragmatic eventration. *Clin. Perinatol.* **44(4)**, 773–779.
- Cossart, Y. E., Field, A. M., Cant, B., Widdows, D. (1975) Parvovirus-like particles in human sera. *Lancet* **1(7898)**, 72–73.
- Di Domenico, C., Moschese, V., Chini, L., Zirletta, E., Cancrini, C., Di Paolo, A., Rossi, P., Scalamandrè, A. (2002) Perinatal infections of B19 parvoviruses. *Ig. Sanita Pubbl.* **LVIII(3)**, 155–162. (in Italian)
- Faure, J. M., Giacalone, P. L., Deschamps, F., Boulot, P. (1996) Nonimmune hydrops fetalis caused by intrauterine human parvovirus B19 infection: A case of spontaneous reversal in utero. *Fetal Diagn. Ther.* **12(2)**, 66–67.
- Gratacós, E., Torres, P. J., Vidal, J., Antolín, E., Costa, J., Jiménez de Anta, M. T., Cararach, V., Alonso, P. L., Fortuny, A. (1995) The incidence of human parvovirus B19 infection during pregnancy and its impact on perinatal outcome. *J. Infect. Dis.* **171(5)**, 1360–1363.
- Hartwig, N. G., Vermeij-Keers, C., Van Elsacker-Niele, A. M., Fleuren, G. J. (1989) Embryonic malformations in a case of intrauterine parvovirus B19 infection. *Teratology* **39(3)**, 295–302.
- Heegaard, E. D., Brown, K. E. (2002) Human parvovirus B19. *Clin. Microbiol. Rev.* **15(3)**, 485–505.
- Kerr, J. R., O'Neill, H. J., Coyle, P. V., Thompson, W. (1994) An outbreak of parvovirus B19 infection; A study of clinical manifestations and the incidence of fetal loss. *Ir. J. Med. Sci.* **163(2)**, 65–67.
- Konstantinidou, A. E., Syridou, G., Spanakis, N., Tsakris, A., Agrogiannis, G., Patsouris, E. (2007) Association of hypospadias and cardiac defect in a parvovirus B19-infected stillborn: A causality relation? *J. Infect.* **54(1)**, e41–e45.
- Maeda, H., Shimokawa, H., Satoh, S., Nakano, H., Nunoue, T. (1988) Nonimmunologic hydrops fetalis resulting from intrauterine human parvovirus B-19 infection: Report of two cases. *Obstet. Gynecol.* **72(3 Pt 2)**, 482–485.
- Makhseed, M., Pacsa, A., Ahmed, M. A., Essa, S. S. (1999) Pattern of parvovirus B 19 infection during different trimesters of pregnancy in Kuwait. *Infect. Dis. Obstet. Gynecol.* **7(6)**, 287–292.
- Masini, L., Apicella, M., De Luca, C., Valentini, P., Manfredi, R., Lanzone, A., De Santis, M. (2017) Fetal central nervous system and infectious diseases. *Donald School J. Ultrasound Obstet. Gynecol.* **11(4)**, 314–327.
- Matsunaga, Y., Matsukura, T., Yamazaki, S., Sugase, M., Izumi, R. (1987) Hydrops fetalis caused by intrauterine human parvovirus infection. *Jpn. J. Med. Sci. Biol.* **40(4)**, 165–169.
- Mielke, G., Enders, G. (1996) Late onset of hydrops fetalis following intrauterine parvovirus B19 infection. *Fetal Diagn. Ther.* **12(1)**, 40–42.
- Nyman, M., Tolfvenstam, T., Petersson, K., Krassny, C., Skjöldebrand-Sparre, L., Broliden, K. (2002) Detection of human parvovirus B19 infection in first-trimester fetal loss. *Obstet. Gynecol.* **99(5 Pt 1)**, 795–798.
- Ornoy, A., Ergaz, Z. (2017) Parvovirus B19 infection during pregnancy and risks to the fetus. *Birth Defects Res.* **109(5)**, 311–323.
- Pradhan, P., Karmacharya, R. M., Vaidya, S., Singh, A. K., Thapa, P., Dhakal, P., Dahal, S., Bade, S., Bhandari, N. (2020) Case report of eventration of diaphragm due to an unknown febrile illness causing phrenic nerve palsy and other multiple nerve palsies. *Ann. Med. Surg. (Lond.)* **54**, 74–78.
- Rossi, A., Delabaere, A., Delmas-Laurichesse, H., Beaufrière, A. M., Lémery, D., Gallot, D. (2014) The challenge of prenatal identification of congenital diaphragmatic hernia in the context of hydrops. *Eur. J. Obstet. Gynecol. Reprod. Biol.* **182**, 238–239.
- Sahakian, V., Weiner, C. P., Naides, S. J., Williamson, R. A., Scharosch, L. L. (1991) Intrauterine transfusion treatment of nonimmune hydrops fetalis secondary to human parvovirus B19 infection. *Am. J. Obstet. Gynecol.* **164(4)**, 1090–1091.

- Saleh, M., Suwaid, M., Idris, S., Tabari, A., Isyaku, K. (2012) Diaphragmatic eventration mimicking congenital diaphragmatic hernia: The value of chest radiograph and barium meal in diagnosis. *Niger. J. Basic Clin. Sci.* **9(1)**, 36–39.
- Schumpelick, V., Steinau, G., Schlüper, I., Prescher, A. (2000) Surgical embryology and anatomy of the diaphragm with surgical applications. *Surg. Clin. North Am.* **80(1)**, 213–239, xi.
- Shojai, R., Gire, C., Chaumoitre, K., Merrot, T., Panuel, M., Boubli, L., D'Ercole, C. (2004) Right diaphragmatic hernia and hydrops: Is it always fatal? *Ultrasound Obstet. Gynecol.* **24(7)**, 803–804.
- Soni, A., Singh, P., Singh, R., Sood, V. (2005) Eventration of diaphragm – Embryologic basis. *J. Anat. Soc. India* **54(2)**, 1–9.
- Sydorak, R. M., Goldstein, R., Hirose, S., Tsao, K., Farmer, D. L., Lee, H., Harrison, M. R., Albanese, C. T. (2002) Congenital diaphragmatic hernia and hydrops: A lethal association? *J. Pediatr. Surg.* **37(12)**, 1678–1680.
- Tarver, R. D., Godwin, J. D., Putman, C. E. (1984) Symposium on Nonpulmonary Aspects in Chest Radiology. The diaphragm. *Radiol. Clin. North Am.* **22(3)**, 615–631.
- Tiessen, R. G., van Elsacker-Niele, A. M., Vermeij-Keers, C., Oepkes, D., van Roosmalen, J., Gorsira, M. C. (1994) A fetus with a parvovirus B19 infection and congenital anomalies. *Prenat. Diagn.* **14(3)**, 173–176.
- Tolfvenstam, T., Papadogiannakis, N., Norbeck, O., Petersson, K., Broliden, K. (2001) Frequency of human parvovirus B19 infection in intrauterine fetal death. *Lancet* **357(9267)**, 1494–1497.
- Woernle, C. H., Anderson, L. J., Tattersall, P., Davison, J. M. (1987) Human parvovirus B19 infection during pregnancy. *J. Infect. Dis.* **156(1)**, 17–20.
- Yaegashi, N., Okamura, K., Yajima, A., Murai, C., Sugamura, K. (1994) The frequency of human parvovirus B19 infection in nonimmune hydrops fetalis. *J. Perinat. Med.* **22(2)**, 159–163.

# Instructions to Authors

Prague Medical Report is an English multidisciplinary biomedical journal published quarterly by the First Faculty of Medicine of the Charles University. Prague Medical Report (Prague Med Rep) is indexed and abstracted by Index-medicus, MEDLINE, PubMed, EuroPub, CNKI, DOAJ, EBSCO, and Scopus.

## Articles issued in the journal

- a) Primary scientific studies on the medical topics (not exceeding 30 pages in standardized A4 format – i.e. 30 lines and 60–65 characters per line – including tables, graphs or illustrations)
- b) Short communications
- c) Case reports
- d) Reviews
- e) Lectures or discourses of great interest
- f) Information about activities of the First Faculty of Medicine and other associated medical or biological organizations

## Layout of the manuscript

- a) Title of the study (brief and concise, without abbreviations)
- b) Information about the author(s) in the following form:
  - first name and surname of the author(s) (without scientific titles)
  - institution(s) represented by the author(s)
  - full corresponding (mailing) author's reference address (including first name, surname and scientific titles, postal code, phone/fax number and e-mail)
- c) Abstract (maximum 250 words)
- d) Key words (4–6 terms)
- e) Running title (reduced title of the article that will appear at the footer (page break), not more than 50 typewritten characters including spaces)
- f) Introduction
  - The use of abbreviations should be restricted to SI symbols and those recommended by the IUPAC-IUB. Abbreviations should be defined in brackets on first appearance in the text. Standard units of measurements and chemical symbols of elements may be used without definition.
- g) Material and Methods
- h) Results
- i) Discussion

## j) Conclusion

## k) References

- All the sources of relevant information for the study should be cited in the text (citations such as “personal communication” or “confidential data” are not accepted).
  - It is not permitted to cite any abstract in the References list.
  - References should be listed alphabetically at the end of the paper and typed double-spaced on separate pages. First and last page numbers must be given. Journal names should be abbreviated according to the Chemical Abstract Service Source Index. All co-authors should be listed in each reference (et al. cannot be used).
  - Examples of the style to be used are:  
Yokoyama, K., Gachelin, G. (1991) An Abnormal signal transduction pathway in CD4–CD8– double-negative lymph node cells of MRL *lpr/lpr* mice. *Eur. J. Immunol.* **21**, 2987–2992.  
Lloyd, D., Poole, R. K., Edwards, S. W. (1992) *The Cell Division Cycle. Temporal Organization and Control of Cellular Growth and Reproduction*. Academic Press, London.  
Teich, N. (1984) Taxonomy of retroviruses. In: *RNA Tumor Viruses*, eds. Weiss, R., Teich, N., Varmus, H., Coffin, J., pp. 25–207, Cold Spring Harbor Laboratory, Cold Spring Harbor, New York.
- References in the text should be cited as follows: two authors, Smith and Brown (1984) or (Smith and Brown, 1984); three or more authors, Smith et al. (1984) or (Smith et al., 1984). Reference to papers by the same author(s) in the same year should be distinguished in the text and in the reference list by lower-case letters, e.g. 1980a, or 1980a, b.

## l) tables, figures, illustrations, graphs, diagrams, photographs, etc. (incl. legends)

**Technical instructions**

- a) Manuscripts (in UK English only) must be delivered in the electronic form via Online Manuscript Submission and Tracking system (<http://www.praguemedicalreport.org/>). In case of problems, contact the Prague Medical Report Office ([medical.report@lf1.cuni.cz](mailto:medical.report@lf1.cuni.cz)). The online submission has to include the complete version of the article in PDF format, separately the manuscript as a MS Word file and a cover letter. The detailed version of the Instructions to Authors can be found at: [http://www.praguemedicalreport.org/download/instructions\\_to\\_authors.pdf](http://www.praguemedicalreport.org/download/instructions_to_authors.pdf).
- b) Text should be written in MS WORD only. We accept only documents that have been spell-checked with UK English as a default language.
- c) Please, write your text in Times New Roman script, size 12, and line spacing 1.5.
- d) Text should be justified to the left, with no paragraph indent (use Enter key only); do not centre any headings or subheadings.

- e) Document must be paginated-numbered beginning with the title page.
- f) Tables and graphs should represent extra files, and must be paginated too.
- g) Edit tables in the following way: Make a plain text, indent by Tab (arrow key) all the data belonging to a line and finish the line by Enter key. For all the notes in table, use letter x, not \*.
- h) Make your graphs only in black-and-white. Deliver them in electronic form in TIFF or JPG format only.
- i) Deliver illustrations and pictures (in black-and-white) in TIFF or JPG format only. The coloured print is possible and paid after agreement with the Prague Medical Report Office.
- j) Mark all the pictures with numbers; corresponding legend(s) should be delivered in an extra file. Mark the position of every picture (photo) in the manuscript by the corresponding number, keep the order 1, 2, 3...

### **Authors' Declaration**

The corresponding (or first author) of the manuscript must print, fill and sign by his/her own hand the Authors Declaration and fax it (or send by post) to the Prague Medical Report Office. Manuscript without this Declaration cannot be published. The Authors' Declaration can be found by visiting our web pages: <http://pmr.lf1.cuni.cz> or web pages of Prague Medical Report Online Manuscript Submission and Tracking system: <http://www.praguemedicalreport.org/>.

### **Editorial procedure**

Each manuscript is evaluated by the editorial board and by a standard referee (at least two expert reviews are required). After the assessment the author is informed about the result. In the case the referee requires major revision of the manuscript, it will be sent back to the author to make the changes. The final version of the manuscript undergoes language revision and together with other manuscripts, it is processed for printing.

Concurrently, proofs are electronically sent (in PDF format) to the corresponding (mailing) author. Author is to make the proofs in PDF paper copy and deliver it back to the editorial office by fax or as a scanned file by e-mail. Everything should be done in the required time. Only corrections of serious errors, grammatical mistakes and misprints can be accepted. More extensive changes of the manuscript, inscriptions or overwriting cannot be accepted and will be disregarded. Proofs that are not delivered back in time cannot be accepted.

### **Article processing charge**

Authors do not pay any article processing charge.

### **Open Access Statement**

This is an open access journal which means that all content is freely available without charge to the user or his/her institution. Users are allowed to read, download, copy,

distribute, print, search, or link to the full texts of the articles, or use them for any other lawful purpose, without asking prior permission from the publisher or the author. This is in accordance with the BOAI definition of open access.

### **Copyright Statement**

The journal applies the Creative Commons Attribution 4.0 International License to articles and other works we publish. If you submit your paper for publication by Prague Medical Report, you agree to have the CC BY license applied to your work. The journal allows the author(s) to hold the copyright without restrictions.

Editorial Office

Prague Medical Report

Kateřinská 32, 121 08 Prague 2, Czech Republic

e-mail: [medical.report@lf1.cuni.cz](mailto:medical.report@lf1.cuni.cz)

Phone: +420 224 964 570. Fax: +420 224 964 574

# Prague Medical REPORT

(Sborník lékařský)

Published by the First Faculty of Medicine, Charles University, Karolinum Press,  
Ovocný trh 560/5, 116 36 Praha 1 – Staré Město, Czech Republic, [www.karolinum.cz](http://www.karolinum.cz)

*Editorial Office:* Prague Medical Report, Kateřinská 32, 121 08 Prague 2, Czech Republic,  
Phone: +420 224 964 570, Fax: +420 224 964 574,

e-mail: [medical.report@lf1.cuni.cz](mailto:medical.report@lf1.cuni.cz)

*Editor in Chief:* Kateřina Jandová, MD., PhD.

*Foreign Language Editor:* Prof. Jaroslav Pokorný, MD., DSc.

*Executive Editor:* Mgr. Lucie Šulcová

*Editorial Board:* Prof. Jan Betka, MD., DSc.; Zdeněk Kostrouch, MD., PhD.;

Prof. Emanuel Nečas, MD., DSc.; Prof. Karel Smetana, MD., DSc.;

Prof. Karel Šonka, MD., DSc.; Assoc. Prof. Jan Tošovský, MD., PhD.;

Prof. Jiří Zeman, MD., DSc.

Published as quarterly journal. Typeset and printed by Karolinum Press.

Annual subscription (4 issues) EUR 60,–. Single copy EUR 20,–.

Distribution: Karolinum Press, Ovocný trh 560/5,

116 36 Praha 1, Czech Republic, e-mail: [journals@karolinum.cz](mailto:journals@karolinum.cz)

ISSN 1214-6994 (Print)

ISSN 2336-2936 (Online)

Reg. No. MK ČR E 796